

CHALMERS



Energy Management Strategies for Plug-in Hybrid Electric Vehicles

Master of Science Thesis

Henrik Fridén

Hanna Sahlin

Department of Signals and Systems

Division of Automatic Control, Automation and Mechatronics

CHALMERS UNIVERSITY OF TECHNOLOGY

Göteborg, Sweden 2012

Report No. EX043/2012

THESIS FOR THE DEGREE OF MASTER IN SCIENCE

Energy Management Strategies for Plug-in
Hybrid Electric Vehicles

Henrik Fridén
Hanna Sahlin

Department of Signals and Systems
CHALMERS UNIVERSITY OF TECHNOLOGY

Göteborg, Sweden 2012

Energy Management Strategies for Plug-in Hybrid Electric Vehicles

Henrik Fridén

Hanna Sahlin

©Henrik Fridén, Hanna Sahlin, 2012

Master of Science Thesis in cooperation with Volvo Car Corporation

Report No. EX043/2012

Department of Signals and Systems

Chalmers University of Technology

SE-412 96 Göteborg

Sweden

Telephone: + 46 (0)31-772 1000

Cover:

Energy Management Strategies for Plug-in Hybrid Electric Vehicles

Chalmers Reproservice

Göteborg, Sweden 2012

Abstract

Along with the common goal of reducing fuel consumption for vehicles, the hybrid electric vehicle stands out as a mean for more fuel efficient driving. Besides the conventional combustion engine and fuel tank, the hybrid electric vehicle is also equipped with an electric motor and a battery for propulsion. Car manufacturers are presently working to provide the markets with the next step of this concept, the plug-in hybrid electric vehicle, allowing the on-board battery to be recharged from the power grid.

The aim of this master thesis is to evaluate two different energy management strategies for plug-in hybrid electric vehicles. These energy management strategies consist of both *control* strategies as well as *battery discharge* strategies.

This thesis evaluates an already existing control strategy based on rules for energy management. It also involves MATLAB® and Simulink® implementation of a control strategy; the Equivalent Consumption Minimization Strategy (ECMS), which is based on the concept of optimal control. ECMS operates by continuous evaluation of the fuel consumption cost for different power splits as a basis for selecting the most fuel efficient operating point between the internal combustion engine and the electric motor.

Two battery discharge strategies have been investigated. The first one is the Charge Depletion Charge Sustaining (CDCS) strategy, depleting the battery in an all-electric drive first and then operating in sustaining mode. The other method is to blend the use of the electric motor with the combustion engine at various points throughout the entire trip in a blended mode discharge strategy.

A comparison has been made between a rule-based control strategy with CDCS and the ECMS control strategy for both blended and CDCS discharge. The comparison is done with respect to fuel consumption but side effects related to the battery power usage are observed as well. It is concluded that fuel consumption using ECMS with a blended discharge can be reduced by 4.2 % on average and by 1.0 % on average for CDCS discharge, compared to using the rule-based control strategy with CDCS. Battery power losses are reduced by 15.6 % under a blended discharge strategy and by 7.9 % for CDCS discharge.

Keywords: Plug-in hybrid electric vehicle, ECMS, Optimal control, Charge Depletion Charge Sustaining, Blended discharge, Discharge strategies, Control strategies, Energy Management, Fuel consumption minimization.

Preface

This master thesis project was carried out during the spring of 2012 at Volvo Car Corporation, department of Complete powertrain located in Göteborg, Sweden and at Chalmers University of Technology, department of Signals and Systems, division of Automatic Control, Automation and Mechatronics.

We would like to thank our supervisor Anders Lasson at Volvo Car Cooperation for the support and valuable insight throughout this thesis project. Secondly, great thanks goes to our supervisor Viktor Larsson at Chalmers University of Technology, for guidance and quality discussions. We would also like to extend our thanks to our examiner Professor Bo Egardt for the questions and experience you have shared with us during the project.

Henrik and Hanna
Göteborg, June 2012

Abbreviations

| | |
|------|--|
| AER | All Electric Range |
| CDCS | Charge Depletion Charge Sustaining |
| ECMS | Equivalent Consumption Minimization Strategy |
| ECU | Electric Control Unit |
| EM | Electric Motor |
| EMS | Energy Management System |
| GB | Gearbox |
| ICE | Internal Combustion Engine |
| ISG | Integrated Starter Generator |
| HEV | Hybrid Electric Vehicle |
| NEDC | New European Drive Cycle |
| PHEV | Plug-in Hybrid Electric Vehicle |
| RMS | Root Mean Square |
| SoC | State of Charge |

Physical parameters

Notations of the physical parameters with their units

| | |
|------------------|---|
| ρ_{air} | Density of air, [kg/m^3] |
| $\eta_{gr,EM}$ | Efficiency of the gear between the electrical motor and the rear wheels |
| $\eta_{gr,belt}$ | Efficiency of the belt connection between the ICE and the ISG |
| A_f | Front area, [m^2] |
| C_d | Air dynamic drag resistance |
| D_{tot} | Estimated trip distance, [m] |
| f_r | Rolling resistance coefficient |
| g | Acceleration of gravity, [m/s^2] |
| gr_{EM} | Gear ratio between the electric motor and the rear wheels |
| gr_{belt} | Gear ratio of the belt connection between the ICE and the ISG |
| m | Vehicle mass, [kg] |
| P_{aux} | Auxiliary power, [W] |
| r_{whl} | Wheel radius, [m] |
| Q | Electric charge capacity, [C] |
| Q_{lhv} | Lower heating value, [J/kg] |
| SoC_{final} | Final State of Charge, [%] |
| SoC_{init} | Initial State of Charge, [%] |

Physical variables

Notations of the physical variables with their units

| | |
|------------------|---|
| ω_{whl} | Wheel angular velocity, $[rad/s]$ |
| ω_{EM} | EM angular velocity, $[rad/s]$ |
| ω_{CrSh} | Crankshaft angular velocity, $[rad/s]$ |
| ω_{ISG} | ISG angular velocity, $[rad/s]$ |
| θ | Road grade, $[rad]$ |
| d | Currently traveled distance, $[m]$ |
| F_{drive} | Drive force of the vehicle, $[N]$ |
| F_{drag} | Drag force of the vehicle, $[N]$ |
| F_{roll} | Rolling resistance force of the vehicle, $[N]$ |
| F_{grade} | Road grade force of the vehicle, $[N]$ |
| gr_{GB} | Gearbox ratio between crankshaft and front wheels |
| i | Battery current, $[A]$ |
| \dot{m}_{fuel} | Fuel mass flow, $[kg/s]$ |
| R_{batt} | Battery resistance, $[\Omega]$ |
| P_{batt} | Battery power, $[W]$ |
| $P_{batt,loss}$ | Battery losses, $[W]$ |
| $P_{EM,El}$ | Total EM power, $[W]$ |
| $P_{EM,mech}$ | Mechanical EM power, $[W]$ |
| $P_{fuel,ICE}$ | ICE fuel power, $[W]$ |
| P_{fuel} | Total fuel power, $[W]$ |
| $P_{ISG,El}$ | ISG total power $[W]$ |
| $P_{loss,El}$ | Electrical power losses, $[W]$ |
| $P_{loss,mech}$ | EM mechanical power losses, $[W]$ |
| SoC_{ref} | State of Charge reference, $[\%]$ |
| SoC | Current State of Charge, $[\%]$ |
| $T_{EM,whl}$ | EM torque seen at the wheels, $[Nm]$ |
| T_{EM} | EM torque seen at the motor, $[Nm]$ |
| $T_{CrSh,whl}$ | Crankshaft torque seen at the wheels, $[Nm]$ |
| T_{CrSh} | Crankshaft torque, $[Nm]$ |
| T_{ICE} | ICE torque seen at the engine, $[Nm]$ |
| T_{ISG} | ISG torque seen at the shaft, $[Nm]$ |
| T_{whl} | Requested torque at the wheels, $[Nm]$ |
| V_{batt} | Battery voltage, $[V]$ |
| v | Velocity, $[m/s]$ |

Contents

| | |
|--|------------|
| Abstract | i |
| Preface | ii |
| Abbreviation | iii |
| Physical parameters | iii |
| Physical variables | iii |
| Contents | v |
| 1 Introduction | 1 |
| 1.1 Project background | 1 |
| 1.2 Aim | 2 |
| 1.3 Exclusions | 3 |
| 1.4 Objectives | 3 |
| 1.5 Outline | 3 |
| 2 The Hybrid Electric Vehicle | 5 |
| 2.1 Powertrain configurations | 6 |
| 2.2 Investigated powertrain configuration | 8 |
| 3 Vehicle model | 11 |
| 3.1 Dynamic powertrain model | 11 |
| 3.2 Simplified powertrain model | 13 |
| 3.2.1 Drive system power flows | 15 |
| 3.2.2 Power split ratio | 17 |
| 3.3 Battery model | 18 |
| 4 The energy management problem | 21 |
| 4.1 Rule-based control strategy | 21 |
| 4.2 Discharge strategies | 21 |
| 4.3 Optimal control | 23 |
| 4.4 Equivalent Consumption Minimization Strategy | 23 |
| 5 Implementation of ECMS | 27 |
| 5.1 Stating the cost function | 27 |
| 5.2 Engine startup cost | 28 |
| 5.3 Determining the equivalence factor | 29 |
| 5.4 Implementing the ECMS algorithm | 34 |

| | | |
|-----------|---|------------|
| 6 | Results | 37 |
| 6.1 | Equivalence factor | 37 |
| 6.2 | Start penalty | 38 |
| 6.3 | ECMS performance | 40 |
| 7 | Analysis | 49 |
| 7.1 | Fuel consumption | 49 |
| 7.2 | Engine start cost | 49 |
| 7.3 | Battery operation | 50 |
| 7.4 | Drive cycle influence | 50 |
| 7.5 | Equivalence factor | 51 |
| 8 | Discussion | 53 |
| 8.1 | Reducing the fuel consumption | 53 |
| 8.2 | Battery life | 53 |
| 8.3 | Modeling errors | 54 |
| 8.4 | Estimation of equivalence factor | 55 |
| 8.5 | Estimation errors | 55 |
| 9 | Future work | 57 |
| 9.1 | Better engine start cost | 57 |
| 9.2 | Mechanical energy reference | 57 |
| 9.3 | Route recognition | 57 |
| 9.4 | ECMS model update | 58 |
| 9.5 | ECU implementation | 58 |
| 10 | Conclusions | 59 |
| | References | 61 |
| | Appendices | I |
| A | Drive cycles | I |
| B | List of inputs and constants to the ECMS algorithm | V |
| C | The variation of $s(t)$ | VII |

1 Introduction

In times of frequent debate regarding the price, peak production, politics and secure delivery of oil as well as if or how to best prevent climate change, the much oil associated automotive industry is consequently handed a list of matters to consider. One way of decreasing the fossil fuel dependency of vehicles is to use a different energy source for their propulsion. A Hybrid Electric Vehicle (HEV) is based upon a conventional vehicle powertrain with an Internal Combustion Engine (ICE) and fuel tank, but with the addition of an Electric Motor (EM) and a secondary energy storage in the form of an electric battery. The main purpose of a HEV is to save fuel, which is done by partially using the EM for propulsion and regenerative braking (to charge the battery). A more recent development from the HEV is the *Plug-in* Hybrid Electric Vehicle (PHEV) which introduces the ability to charge the battery externally, from the grid, before the trip and then leaving it depleted at the end. Doing so allows for larger potential savings in fuel consumption, especially since the battery size is usually selected larger for a PHEV. A larger battery increases the *All Electric Range* (AER) of the vehicle, allowing it to drive further distances while only consuming electric energy. For a more detailed description of the hybrid vehicle concept, see Section 2.

According to [1] and [2], about half of all trips made in Sweden (by any means of transportation) are work related, and the average distance to work is 16 km. This suggests that even a modestly sized battery for a PHEV may have a significant impact on fuel consumption and carbon dioxide emissions by allowing all-electric driving for a large part of the daily trips. When it comes to “well-to-wheel” emissions, it is important to consider how the grid electricity is produced.

The commercialization of PHEVs is still in an early stage with the earliest launches in 2010 and many more to come in 2012. This may suggest that there is plenty of room for improvement and optimization with respect to fuel consumption as academia findings are being bridged into the industry. One such area is within the *Energy Management System* (EMS) of the vehicle, whose task is to control the power split between the ICE and the EM in order to achieve an efficient energy usage.

1.1 Project background

Volvo Car Corporation is in the process of developing a PHEV for commercial use. The EMS used to control the powertrain is employing a *Charge Depletion Charge Sustaining* (CDCS) battery discharge strategy by applying a set of rules to decide conditions for battery discharge. This strategy may also be referred to as the *nominal* strategy throughout this thesis, simply because it is the one to which comparisons are made. Essentially CDCS implies that the EM stands for all propulsion in a Charge Depletion mode (CD) until battery charge is low, after which the ICE performs most of the propulsion in a Charge Sustaining (CS) mode for the remainder of the trip. The CS mode makes sure to keep a minimum level of battery charge, and may involve occasional electric propulsion if enough energy

is regenerated from braking. An alternative to this particular discharge strategy is to use the battery more evenly over the entire trip. This is referred to as *blended* mode driving simply because it blends fuel and battery usage. See Figure 1.1 for an illustration of the two discharge strategies.

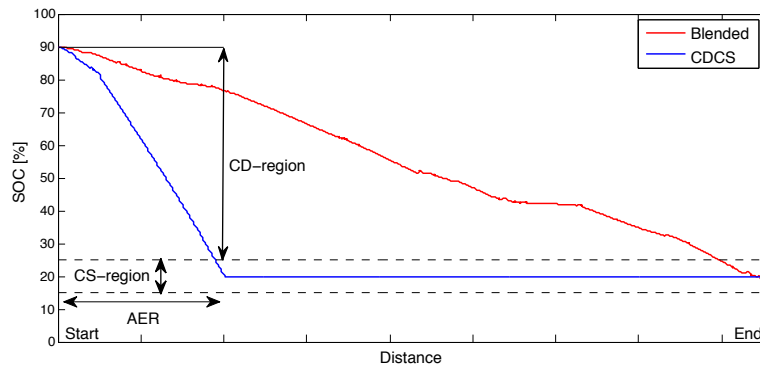


Figure 1.1: Illustrations of typical characteristics of the two discharge strategies. The CS segment of the CDCS strategy seems flat, but does in practice fluctuate within the CS-region as energy from regenerative braking is charged and consumed along the trip.

Studies have shown that it may be possible to reduce the relative fuel consumption by 1-4 % by using a blended discharge strategy for trips exceeding the AER of the vehicle [3], compared to the CDCS strategy. A blended discharge strategy can be realized by a control method such as *Equivalent Consumption Minimization Strategy* (ECMS) [4], [5]. The principle of ECMS is based on, at every time instant, comparing an estimated cost of fuel and electricity consumption when deciding the power split between ICE and EM propulsion. With the cost as a basis, other conditions such as battery level and trip distance apply, which may be used to manipulate the *perceived* cost of propulsion. The lowest perceived cost is then what decides the power split of the ICE and EM. Section 4.4 contains a more detailed description of ECMS. In comparison to much of the literature, which commonly investigates the ECMS control strategy for more simplified vehicle models, this thesis aims for an evaluation of ECMS using a more thorough and comprehensive model with multiple dynamic states.

1.2 Aim

The purpose of the thesis is to implement a blended discharge strategy based on the ECMS control strategy for a dynamic and extensive vehicle model of a PHEV. Under the assumption of a known trip length, the ECMS should be evaluated against a rule-based CDCS discharge strategy, with respect to fuel consumption.

1.3 Exclusions

The purpose of the thesis is not to determine a control strategy for trips with an unknown length. Furthermore, the thesis will not investigate development of algorithms for route recognition as a mean to determine the trip length a priori. No drive cycles with topography will be investigated, i.e only drive cycles with flat ground will be investigated. There will be no considerations taken to emissions such as NO_x , CO_2 , HC and particles while minimizing the fuel consumption. The thesis does not intend to find globally optimal solutions for benchmarking purposes using Dynamic Programming (DP), as this is simply not viable for a model with a significant number of dynamic states.

1.4 Objectives

The central objectives of the project, in order of importance, are to

- Develop and simulate a control strategy, for a pre-built vehicle model, based on ECMS and make comparisons with today's rule-based control strategy. Evaluation with respect to fuel consumption is based on two discharge strategies; blended mode and CDCS.
- Study side-effects such as changes in battery power losses due to different control and discharge strategies.
- Design the control strategy so that it can be implemented as a real-time control system in the energy management system of the vehicle.
- Investigate how the drive cycle layout, with respect to high and low speed segments, affects fuel consumption.

1.5 Outline

This thesis report is started off with a brief overview of different kinds of powertrain configurations for a HEV. The powertrain of the simulated vehicle is then presented with more in-depth detail, including the modeling of its key components; engine, motor and battery. After describing the vehicle model, the energy management problem is presented first in order to form a basis for understanding the ECMS control strategy. After the theory about the ECMS control a more specific description is given of how the vehicle model and ECMS theory are implemented and used to obtain the results. The results chapter begins with the presentation of some parameter tuning and is then followed up by the main results. After a general analysis of the results, some issues and uncertainties are discussed further as well as some suggestions of future work. The report ends with a conclusion of the main findings.

2 The Hybrid Electric Vehicle

Starting from a conventional vehicle with an ICE and fuel tank, the HEV differs mainly on two points; in addition it also has an EM for propulsion and an electric battery for energy storage. See Figure 2.1 for a brief overview of an HEV powertrain.

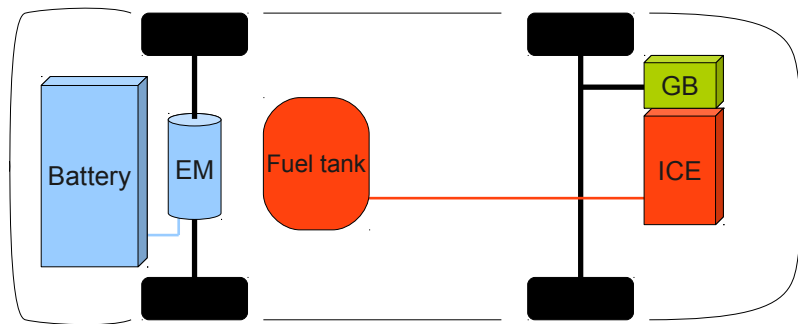


Figure 2.1: An example of an HEV powertrain configuration. The ICE and the EM are capable of propulsion both separately and in parallel to each other.

One of the main benefits that the EM and battery bring is the ability to reuse kinetic energy by regenerative braking. Instead of only using mechanical brakes, the EM is able to alone or partially brake the vehicle by operating as a generator and thus recharging the battery. The HEV concept accounts for two more factors that may reduce fuel consumption. Firstly, it allows for downsizing of the ICE, i.e. making it less powerful, reducing its displacement and thus lowering the instantaneous fuel consumption for a specific operating point. The power reduction is compensated for by the EM as high power demand can still be delivered by assisting the ICE. Secondly, the degree of freedom introduced by the EM can be used to shift the operating point of the ICE. Such shifts could be done successfully by using the EM to assist the ICE in situations where high torque is demanded. Another example is to go by all-electric drive for a low-torque demand, where the ICE efficiency is low and thus avoiding such operating points completely.

An important detail concerning the HEV concept is that the battery charge shall be left at the same level by the end of the trip as in the beginning of the trip. This implies that battery energy may only be “borrowed” during the trip which is quite limiting to how much fuel that can be saved. This is where the PHEV comes in, allowing for a full battery to be completely discharged during a trip and thus allowing for larger savings in fuel.

2.1 Powertrain configurations

For both HEVs and PHEVs, there are three common powertrain configurations; the series, the parallel and the parallel-series powertrain configuration.

The series configuration is presented in Figure 2.2 and as can be seen, the propulsion of the vehicle is done with the EM. The ICE is mechanically decoupled from the wheel axle; instead the engine is coupled to a generator that converts the mechanical energy to electrical energy to either charge the battery or drive the EM. The configuration is considered to be the one closest to a pure electric vehicle [6]. An advantage is that the engine is completely decoupled from the wheels and this results in that the engine operation point can be chosen freely. However, a disadvantage is that all the fuel energy goes through conversion to electricity, involving conversion losses.

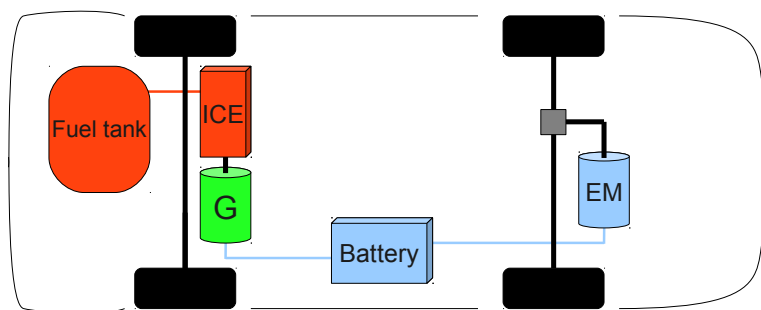


Figure 2.2: A series configuration of the powertrain for a HEV or PHEV. The ICE is mechanically decoupled from the wheels and the EM handles the propulsion.

For the parallel powertrain configuration, both EM and the ICE are mechanically connected to the wheels, which means that both of them can be used for propulsion of the vehicle. The configuration is illustrated in Figure 2.3. Compared to the series configuration, the ICE operation point can not be chosen freely in this type of configuration, which is a disadvantage. The main advantage is that neither of the power sources alone must be sized to meet a peak power demand from the driver, since a combination of the two sources can be used [3].

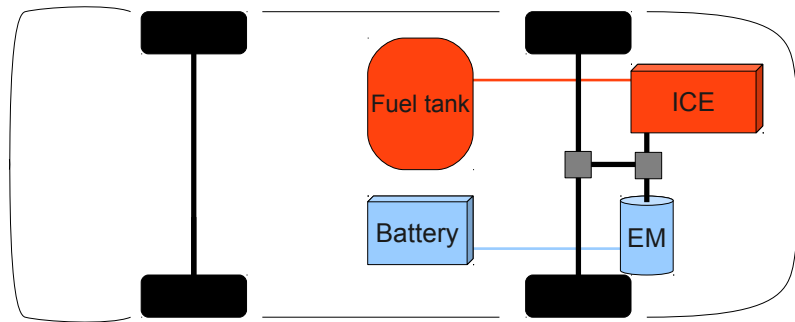


Figure 2.3: A parallel configuration of the powertrain for a HEV or PHEV. The EM and the ICE can be used either separately or together.

The series-parallel powertrain configuration is a combination of the earlier two. This configuration uses a power split device and divides the ICE power between the mechanical path and the electrical path consisting of a generator and an EM, see Figure 2.4. The power split device, often a planetary gear, allows the ICE to some extent to be decoupled from the vehicle speed. It is possible to decide if the engine should be used for propulsion or for charging the battery via the generator [6]. Using the engine for propulsion directly may involve less energy conversion losses compared to the series configuration.

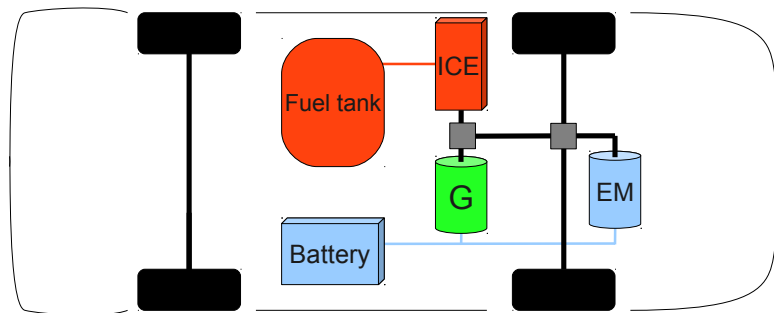


Figure 2.4: A series-parallel configuration of the powertrain for a HEV or PHEV. The power split device is used for allowing different modes of engine operation; idle, battery charging or hybrid propulsion.

2.2 Investigated powertrain configuration

The vehicle treated in this thesis is a medium sized vehicle with specification according to Table 2.1 and is a variant of the parallel hybrid vehicle configuration, with an ICE on the front wheels and EM mounted on the rear wheels. This implies that the motor and engine can operate either separately or simultaneously for propulsion, using their respective energy sources.

Table 2.1: Powertrain specifications for the investigated vehicle.

| Part | Parameter | Value |
|------------------|--|------------------------|
| ICE | max power | 158 kW |
| | max torque | 440 Nm @ 4000 rpm |
| EM | max power | 50 kW |
| | max torque | 200 Nm |
| Battery | cell type | Li-Ion |
| | capacity | 11.2 kWh |
| | voltage, V | 400 V |
| | All Electric Range, AER | ~ 50 km |
| ICE Transmission | type | automatic |
| | number of gears | 6 |
| EM Transmission | gear ratio, gr_{EM} | 9.16 |
| | efficiency, $\eta_{gr,EM}$ | 0.96 |
| ISG Transmission | gear ratio, gr_{belt} | 2.71 |
| | efficiency, η_{belt} | 0.95 |
| Chassis data | mass, m | 2040 kg |
| | drag coefficient · front area, $C_d A_f$ | 0.74 m ² |
| | wheel radius, r_{whl} | 0.3123 m |
| | density of air, ρ_{air} | 1.20 kg/m ³ |
| Fuel | type | diesel |
| | heating value, Q_{lhv} | 42.9 MJ/kg |

The powertrain configuration of the vehicle can be seen in Figure 2.5. The EM is mounted on the rear axle with a fixed gear ratio, gr_{EM} , and with a clutch mounted in series with the motor. When the EM is not in use, for example when the battery charge is too low or the torque demand is too high, the clutch is used for disengaging the EM from the rear wheels. The ICE is mounted in the front together with a gearbox with six gears, where the current gear ratio is denoted gr_{ICE} . The powertrain also contains an Integrated Starter Generator (ISG), which can be used for charging the battery when the charge level is too low or otherwise made a priority. When the ISG is charging, the ICE has to apply some more torque on the crankshaft. The ISG is also used as starter motor if the conditions

for it are satisfied, e.g. if there is sufficient battery charge. To couple the ICE and the ISG there is a belt with a fixed gear ratio gr_{belt} .

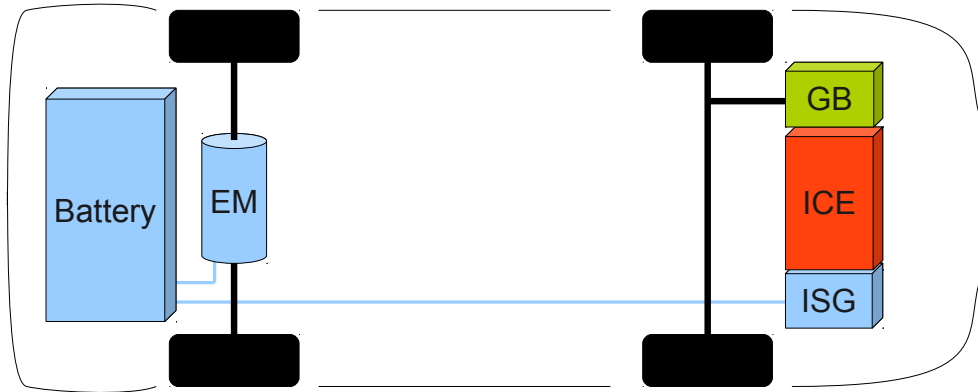


Figure 2.5: The powertrain configuration, consisting of an EM and an ISG for battery charging and an ICE and EM for propulsion. The ISG and ICE are coupled by the crankshaft.

3 Vehicle model

The vehicle model used for simulations is part of Volvo’s own vehicle simulation environment, VSim, a toolbox for MATLAB® and Simulink®. VSim simulates the dynamics of vehicles and their subsystems along a one dimensional road trajectory based on speed profile and time inputs. The vehicle model is quite extensive and complex, accounting for the dynamics of many internal states. A model of such complexity is not suitable for real-time control algorithms if its full functionality is accounted for, simply due to the amount of computing power necessary. Therefore a simplified version of the model is needed that only takes the important states into account, without accounting for their dynamics. In this chapter the complex VSim model is briefly explained as well as its relation to energy management. The simplified model used for the decision based on ECMS is presented in more detail, with the assumptions and simplifications made.

3.1 Dynamic powertrain model

The VSim model simulates multiple processes and their respective control systems from a speed profile input to a vehicle movement output. For a brief overview of this process, see Figure 3.1. Based on the speed profile, requested torque T_{whl} and speed, ω_{whl} , are calculated. The driver is modeled by a PID-controller which calculates T_{whl} based on the velocity in the drive cycle. The output of the energy management block consists of the requested torque for the EM, ICE and the ISG, based on demands from the simulated driver. These torques are then limited with respect to drivability and safety, where the limits depend on requested torque, current speed and various other states of the vehicle. When the requested torques have been limited and controlled, the physical model can be simulated and an update of the internal states is performed.

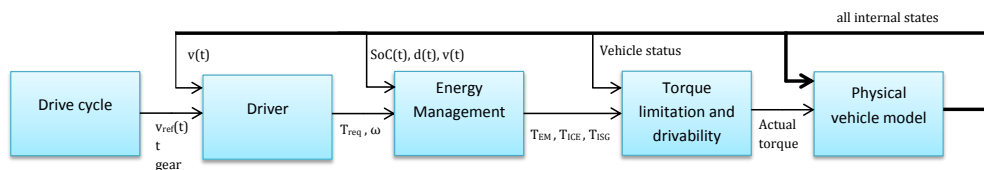


Figure 3.1: Given the inputs, a simulated driver makes torque requests in order to follow the speed profile on which the requested torques have to be controlled and limited for drivability before it is finally applying the actual torques on the wheels. This is done iteratively every simulation time step.

In the VSim model the longitudinal dynamics of the vehicle chassis are modeled according to Newton's second law of motion, where the vehicle is modeled as a point mass

$$m\dot{v}(t) = \underbrace{\frac{T_{whl}(t)}{r_{whl}}}_{F_{drive}} - \left(\underbrace{\left(\frac{\rho_{air}}{2} C_d A_f v(t)^2 \right)}_{F_{drag}} + \underbrace{mg \sin \theta(t)}_{F_{grade}} + \underbrace{f_r mg \cos \theta(t)}_{F_{roll}} \right) \quad (3.1)$$

Here, m is the vehicle mass, T_{whl} is the applied torque on the wheels, r_{whl} is the wheel radius, C_d is the air dynamic drag coefficient, A_f is the front area, v is the velocity of the vehicle, ρ_{air} is the density of air, g is the acceleration of gravity, f_r is the rolling resistance and θ is the road grade [7].

VSim simulates not only the vehicle motion expressed in Equation (3.1) but also various subsystems of the vehicle along with their respective states. Examples include angular speeds for the wheels, the ICE and the EM, all affected by moments of inertia, as well as voltages and currents of electric systems, emissions and temperature. The simulation model also includes the control of various subsystems, for example the engine, brakes, gear shifting, and so on. In Figure 3.2, the structure in VSim with the modeled subsystems for the vehicle is shown. Each subsystem has its own block and by using a bus connection it is possible to communicate with each subsystem. The energy management is a part of the control block with the name *VehSysCtrl* that contains the vehicle propulsion control. This control block consists of acceleration pedal interpretation (calculation of wheel torque request), cruise control, mode shift control (starting/stopping engine), gear selection, etc.

The programming of the Electric Control Units (ECUs) of the actual vehicle is done with a production code generator called TargetLink® [8], which is also from where the control systems are downloaded for Simulink. In that way, the control blocks used for simulations in Simulink match the functionality of the ECUs.

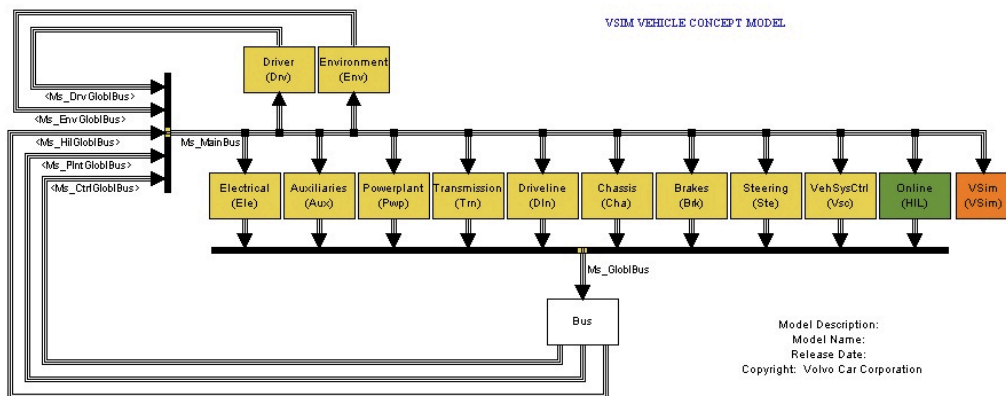


Figure 3.2: A visualization of the true model structure where the energy management is a part of the block called VehSysCtrl that contains the vehicle propulsion control.

3.2 Simplified powertrain model

For the powertrain used in this thesis, with the powertrain configuration as in Section 2.1, a simplified model with the different torques, efficiencies, gear ratios and so on has to be derived to be able to perform the ECMS algorithm. The parameter values in the powertrain can be seen in Table 2.1. Figure 3.3 shows a simplified illustration of the states that the ECMS needs as inputs and the states the algorithm outputs. It can be noted that only a few of the internal states are needed.

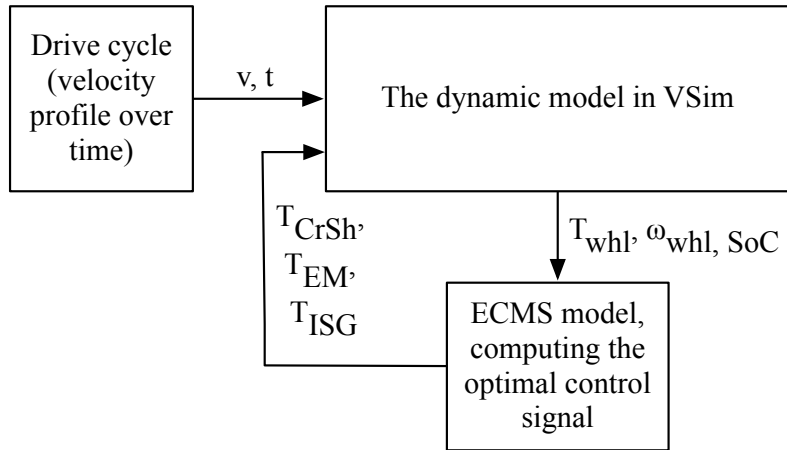


Figure 3.3: A brief presentation of the relation between the dynamic VSim model and the ECMS algorithm where the essential inputs and outputs are displayed.

Based on the torque applied on the wheels, T_{whl} , and the wheel speed, ω_{whl} , it is possible to state the torques that EM, ICE and ISG have to deliver for propulsion of the vehicle. The notations used for the torques and the speeds of the ICE, the EM and the ISG are specified as in Figure 3.4.

The torque that is applied on the crankshaft, T_{CrSh} , of the engine is

$$T_{CrSh} = \frac{T_{CrSh,whl}}{gr_{GB}} \quad (3.2)$$

where gr_{GB} is the gear ratio in the automatic gearbox and $T_{CrSh,whl}$ is the torque at the front wheels, which depends on the requested torque at the wheels from the driver, T_{whl} . The gearbox is assumed ideal for simplicity. The crankshaft speed is denoted by ω_{CrSh} and depends on the wheels speed, ω_{whl} , requested by the driver as

$$\omega_{CrSh} = \omega_{whl} gr_{GB} \quad (3.3)$$

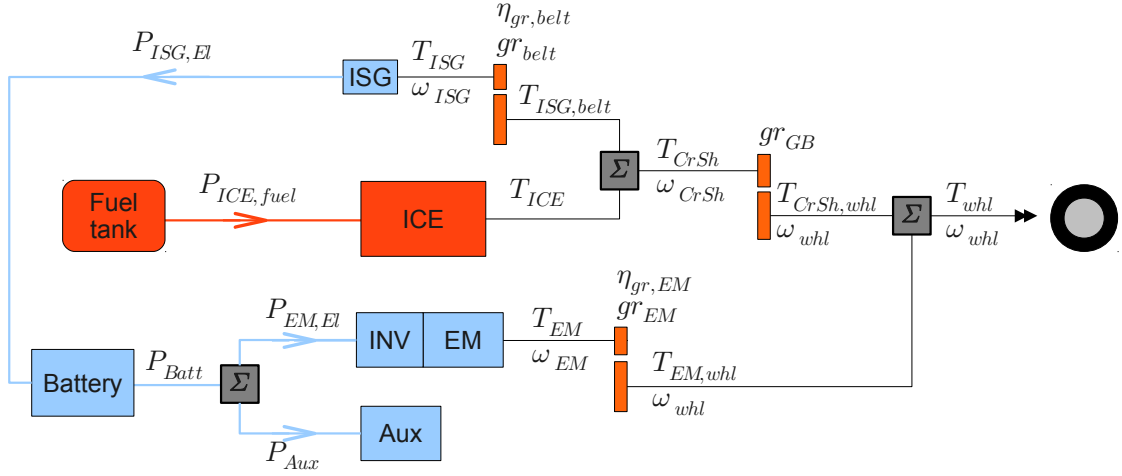


Figure 3.4: The powertrain with the torques, speeds, efficiencies, gears and power flows illustrated.

The torque that has to be applied at the shaft of the ICE, T_{ICE} , is then stated as

$$T_{ICE} = T_{CrSh} - T_{ISG, belt} \quad (3.4)$$

where $T_{ISG, belt}$ is the torque that the ISG requires for extra propulsion on the front wheels, seen at the crankshaft. A negative ISG torque corresponds to charging the battery. The torque that is applied on the ISG shaft, T_{ISG} , is then stated as

$$T_{ISG} = \frac{T_{ISG, belt}}{gr_{belt}} \eta_{belt, 0} \quad (3.5)$$

where gr_{belt} is the gear ratio between the ICEs crankshaft and the ISG which is coupled by a belt. The efficiency of the belt coupling is denoted by $\eta_{belt, 0}$ and depends on if the ISG is used for propulsion or for charging the battery, according to Equation 3.7. The speed of the ISG, ω_{ISG} , is stated as

$$\omega_{ISG} = \omega_{CrSh} gr_{belt} \quad (3.6)$$

The efficiency of the ISG belt coupling depends on whether it is operating as a starter motor or generator, as follows

$$\eta_{belt, 0} = \begin{cases} \frac{1}{\eta_{belt}} & \text{if } T_{ISG} > 0 \\ \eta_{belt} & \text{if } T_{ISG} < 0 \end{cases} \quad (3.7)$$

where η_{belt} is the mechanical efficiency of the ISG belt coupling and $\eta_{belt, 0}$ is the resulting efficiency depending on if the ISG operates as starter motor or generator.

The torque from the EM is denoted as T_{EM} and depends on the torque requested for the wheels and it is calculated as

$$T_{EM} = \frac{T_{EM, whl}}{gr_{EM}} \eta_{gr, EM, 0} \quad (3.8)$$

where $T_{EM,whl}$ is the EM torque at the rear wheels and $\eta_{gr,EM,0}$ is the efficiency that is stated according to Equation 3.10 and depends on if the EM is used for propulsion or regeneration. The gear ratio of the fixed gear is denoted by gr_{EM} . The speed of the EM, ω_{EM} , depends on the wheel speed according to

$$\omega_{EM} = \omega_{whl} gr_{EM} \quad (3.9)$$

The efficiency of the EM path depends on whether it is discharging or charging, as follows

$$\eta_{gr,EM,0} = \begin{cases} \frac{1}{\eta_{gr,EM}} & \text{if } T_{EM} > 0 \\ \eta_{gr,EM} & \text{if } T_{EM} < 0 \end{cases} \quad (3.10)$$

where $\eta_{gr,EM}$ is the mechanical efficiency of the gear and $\eta_{gr,EM,0}$ is the resulting efficiency depending on motor or generator operation.

3.2.1 Drive system power flows

Based on the torques and the different speeds in the system, the different machine's power flow can be stated. The power is later used when deriving the ECMS algorithm and can be seen in Figure 3.4. Starting with the mechanical power for the EM, $P_{EM,mech}$, which can be stated as

$$P_{EM,mech} = T_{EM} \omega_{EM} \quad (3.11)$$

and the mechanical losses, $EM_{loss,mech}$, that is based on a lookup table provided from Volvo Car Corporation and is based on measurements. The input to the lookup table is ω_{EM} and the loss can be denoted as

$$P_{loss,mech} = EM_{loss,mech}(\omega_{EM}) \quad (3.12)$$

There are also EM losses associated with the power electronic inverter, that have to be taken into account when deriving the total power needed from the battery for propulsion. The electrical losses, $P_{loss,El}$, is also based on a lookup table, called $EM_{El,loss}$, and the inputs are T_{EM} , ω_{EM} and also the battery voltage, V_{batt} , as

$$P_{loss,El} = EM_{El,loss}(T_{EM}, \omega_{EM}, V_{batt}) \quad (3.13)$$

Based on these three equations, the total electrical power that the EM consumes from the battery, denoted as $P_{EM,El}$, is then

$$P_{EM,El} = P_{EM,mech} + P_{loss,mech} + P_{loss,El} \quad (3.14)$$

The electric power that is related to the ISG consists of the effective mechanical power and also the electrical losses. The losses are based on a lookup table called $ISG_{loss,El}$ and the inputs to this are T_{ISG} , ω_{ISG} and also the battery voltage V_{batt} .

The mechanical power is calculated based on the torque and the speed of the ISG shaft. The electrical power of the ISG, $P_{ISG,El}$, is stated according to

$$P_{ISG,El} = T_{ISG}\omega_{ISG} + ISG_{loss,El}(T_{ISG},\omega_{ISG},V_{batt}) \quad (3.15)$$

Based on the requested power from the ICE, a resulting fuel mass flow, \dot{m}_{fuel} , is required. The value for \dot{m}_{fuel} is extracted from a lookup table that depends on the torque, T_{ICE} , and the speed, ω_{ICE} . An illustration of this kind of lookup table can be seen in Figure 3.5, where it can be noticed that the combustion engine should operate at high torque to obtain high efficiency, which can be related to a high vehicle velocity. It can be seen that the most efficient operating point is near the maximum torque limit of the ICE. Based on this type of lookup table and the lower heating value, Q_{lhv} , for diesel, presented in Table 2.1, the fuel power for the ICE can be calculated according to

$$P_{fuel,ICE} = \dot{m}_{fuel}(T_{ICE},\omega_{CrSh})Q_{lhv} \quad (3.16)$$

The efficiency for an electric motor can be seen in Figure 3.6, where it can be noted that an electric motor is the most efficient at medium torque, corresponding to a low vehicle velocity. This means that the EM and ICE can complement each other well by mainly operating in different torque regions.

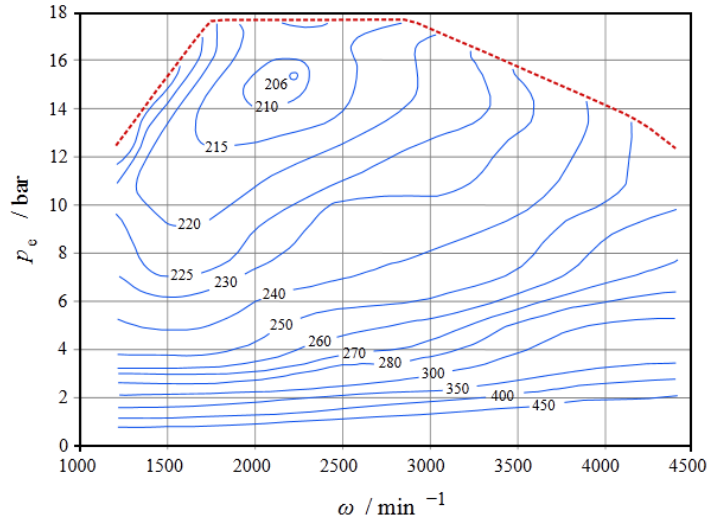


Figure 3.5: Brake specific fuel consumption map for a combustion engine. The quantity p_e denotes the mean effective pressure and is equivalent to the torque supplied by the engine. The contours display the fuel consumption as g/kWh. (Retrieved from Wikimedia Commons under the CC-BY-SA-3.0 license).

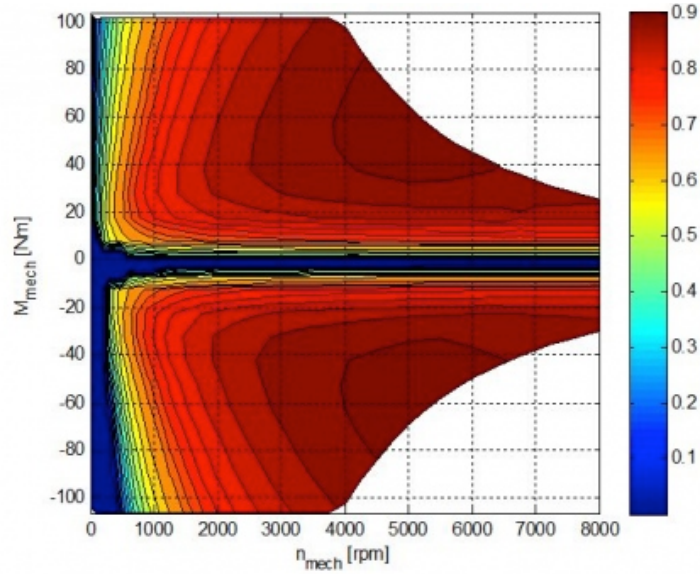


Figure 3.6: Efficiency map for an AC induction motor. Both motoric and generative efficiency are displayed as a function of speed. (Published with permission from Andreas Freuer, University of Stuttgart).

3.2.2 Power split ratio

Based on the previous sections a power split ratio can be defined. This ratio decides how much torque that should be applied on the rear wheels in relation to the front wheels. The vehicle configuration can be regarded as a system with two degrees of freedom and some constraints. Given the requested power it is possible to distribute the load on the front or rear wheels, and subsequently specify the ICE power split ratio between the crankshaft and ISG. Let $\{u_1, u_2\}$ denote the power split ratios according to

$$\begin{cases} u_1 = \frac{T_{EM,whl}}{T_{whl}} \in [0, 1], & \text{for } T_{whl} > 0 \\ u_1 = 1, & \text{for } T_{whl} < 0 \end{cases} \quad (3.17)$$

$$u_2 = \frac{T_{ISG}}{T_{CrSh}} \in [u_{min}, u_{max}] \quad (3.18)$$

When the requested wheel torque T_{whl} is negative, meaning that the driver is braking, the battery should be charged with the brake energy. This means that $u_1 = 1$ every time the driver requests a negative torque. When $u_1 = 1$, with a positive driver request, it corresponds to EM propulsion only and when $u_1 = 0$, it means that only the ICE is used for propulsion. The limits u_{min} and u_{max} , for the power split ratio u_2 , correspond to the minimum and maximum available torque split ratios allowed for charging and for propulsion respectively for the ISG and the ICE. These limits are determined by physical and practical constraints

of the system at each time instant. If u_2 is negative, the ISG is charging while the ICE delivers extra power for charging in addition to propulsion, similar to a conventional engine and generator configuration. If u_2 is positive the ISG will crank the ICE or give the ICE extra torque on the crankshaft when needed. The limits, u_{min} and u_{max} , varies with time. The lower limit can either be a negative value or zero and the higher limit can either be zero or a positive value.

3.3 Battery model

The battery used is of the type Lithium-Ion which can be modeled by a complex chemical model with several dynamic states [3]. Such a model is not practical when it comes to calculating a control strategy in real-time. Instead a less complex model is presented by a simple equivalent circuit, displayed in Figure 3.7. With this simplification, there is only one dynamic state, namely the battery charge level, *State of Charge* (SoC). The SoC is normalized between one and zero, where one means fully charged and zero means depleted. It is assumed that the internal battery resistance, R_{batt} , is constant over the SoC region of normal operation and the open circuit voltage $V_{oc}(SoC)$ is a function of the SoC. Then the battery SoC dynamics can be stated as

$$\frac{dSoC}{dt} = -\frac{i}{Q} = \frac{V_{oc}(SoC) - \sqrt{V_{oc}(SoC)^2 - 4P_{batt}R_{batt}}}{2R_{batt}Q} \quad (3.19)$$

where Q is the nominal capacity of the battery and i is the battery current, defined positive during discharge [9]. P_{batt} is the power drawn by or supplied to the battery terminals and V_{batt} is the voltage at the terminal.

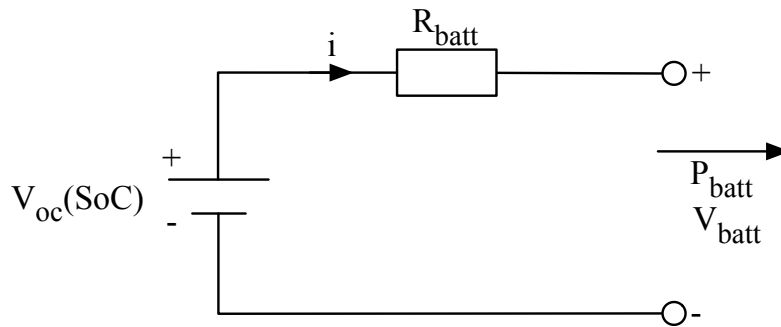


Figure 3.7: An equivalent circuit of the battery where P_{batt} is the power drawn from the battery by the EM and the power electronics in the vehicle. The voltage is the open circuit voltage and depends on the current SoC level. It is assumed that the SoC level is the only varying state in the battery.

In Figure 3.8 a typical open circuit voltage versus SoC characteristic is depicted.

It is assumed that the battery operates in the linear region of the open circuit voltage versus SoC characteristics.

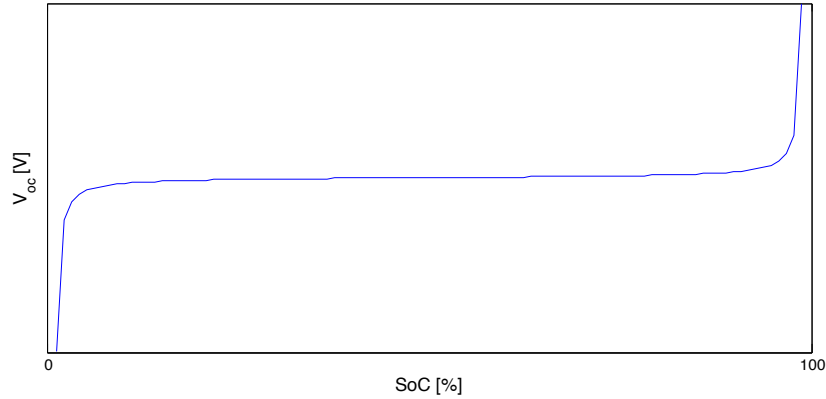


Figure 3.8: Open circuit voltage, V_{oc} versus SoC relationship of a Li-Ion cell. It is assumed that the battery is operated in the linear region where the equivalent circuit also is valid.

A fully charged battery has a higher voltage than a depleted battery. This implies that a fully charged battery operates at a lower current in order to deliver a specific power [10]. The internal losses will then be smaller due to the fact that the battery losses are proportional to the battery current squared and are calculated, based on the electric power that the electric motor require, $P_{EM,El}$, as

$$P_{batt,loss} = R_{batt} \left(\frac{P_{EM,El}}{V_{batt}} \right)^2 \quad (3.20)$$

Since the battery is perhaps the most expensive component in the vehicle, it is desirable to reduce wear and extend the lifetime of it as much as possible. There are several parameters that can affect the lifetime of the battery, e.g. temperature, Ah-throughput (the total cycled current), average time between full charge, the time spent at low SoC level and the cycling rate of the current, just to mention a few of them [11].

4 The energy management problem

The task of the energy management system is to, based on a driver requested torque, determine the power split between the ICE and the EM. The objective is to minimize fuel consumption while still attaining good drivability and low component wear [3]. There are many ways to design the energy management system; a couple of approaches relevant for this work will be described below.

4.1 Rule-based control strategy

A rule-based control strategy for energy management, whose purpose could be to reduce the fuel consumption, is essentially formed upon a set of rules that determine how to use the ICE or EM given some current states. This is the baseline control strategy used in the EMS of the current VSim model. A brief example of how a rule-based controller operates can be seen below

$$ICE_{on/off} = \begin{cases} \text{Off} & \text{if } v_{vehicle} < 50 \text{ km/h,} \\ \text{On} & \text{if } v_{vehicle} > 100 \text{ km/h,} \\ \text{On} & \text{if } T_{Req} > 200 \text{ Nm,} \\ \text{On} & \text{if } SoC < 20 \% \end{cases}$$

There are many rules in the current EMS that control the use of the EM, the ICE and also the ISG. One rule for usage of the ISG is when the current SoC level is too low, below 10 %. Then the battery is charged to a limit where the battery is not harmed. The battery can also be charged if the driver is demanding it, overriding the regular control system. The engine is also turned on if the driver requests a rapid acceleration or otherwise demands high power. When the engine has been turned on, a condition for turning of the engine is specified, it has to be turned on for at least four seconds before it can be turned off. This is to reduce engine wear and may be of significance when designing a control strategy. The EM is used as long as it can supply the wheels with the requested power, if this is not the case the ICE is turned on and the EM is turned off. There are also limits on usage of the EM at high speeds; when the speed of the vehicle is above 100 km/h the engine starts to operate instead of the EM. This is just some of many rules for when to use the ICE, the ISG and the EM.

The different constraints being used vary with vehicle properties and depends on what discharge strategy is being followed. The benefit of a rule-based control strategy is simple implementation and high robustness [5].

4.2 Discharge strategies

Another way to express the objective to minimize fuel consumption is to state that the energy stored in the battery should be used efficiently. One way to achieve this is to impose a certain demand on the discharge pattern of the battery. The discharge pattern can be done in a number of ways. The most efficient way of

discharging the battery from the perspective of minimizing the fuel consumption depends mainly on the trip length. For trips shorter than the AER, only the battery energy should be used, meaning that the optimal discharge strategy is to operate in depletion mode since electric energy is considered to be cheaper for propulsion than fuel. If the trip length exceeds the AER then there are two suggested ways of discharging the battery; either using a CDCS or a blended mode strategy. If the trip length is known a priori, the blended mode discharge strategy has been proven, by using DP, to be the more beneficial discharge strategy of the two [3]. The blended mode strategy consumes the battery energy evenly over the trip at points where it can be used effectively. The benefit with the blended discharge strategy is that the average discharge current is lowered and therefore the power losses can be decreased. This is since the losses are related to the square of the current as presented in Section 3.3. Another benefit with using a blended discharge is that less time is spent in CS mode, which lowers the conversion losses that occurs when current is cycled back and forth through the battery, thanks to a higher voltage and thereby lower currents [3].

If there is no a priori information about the trip, the CDCS discharge strategy is likely to save more fuel since the battery should be depleted by the end of the trip. The battery operates in CD mode until it is empty, then the battery should operate in CS mode. This means, essentially, that the EM should operate during the CD mode and the ICE should operate during the CS mode. If the battery is recharged above a specified threshold during CS mode, then it may resume operation in CD mode again. For a simple comparison of the two discharge strategies, see Figure 4.1. In the figure the SoC_{init} is 90 % and the reference, SoC_{final} , is 20 %, and the threshold to resume CD operation is 25 %.

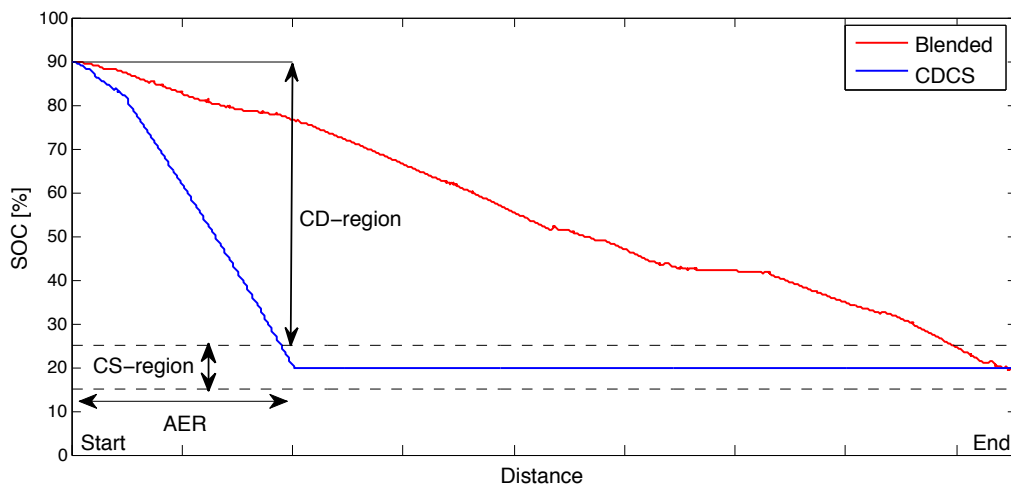


Figure 4.1: SoC trajectory for the two different discharge modes.

4.3 Optimal control

The energy management problem is sometimes formulated as an optimal control problem with the main goal to minimize the fuel cost while respecting the system constraints and specifications [3]. The challenge in this thesis is to minimize the fuel consumption for any given trip while only knowing the trip length. The optimal control problem can be formulated as

$$J^* = \min_u \int_{t_0}^{t_f} \dot{m}_{fuel}(T_{whl}(t), \omega_{whl}(t), x(t), u(t)) dt \quad (4.1)$$

subject to

$$\begin{aligned} \dot{x}(t) &= \frac{dSoC}{dt} \\ SoC(t_0) &= SoC_{init} \\ SoC(t_f) &\geq SoC_{final} \end{aligned} \quad (4.2)$$

Here, $\frac{dSoC}{dt}$ is defined by Equation 3.19, the system state $x(t)$ is the battery SoC that depends on the battery voltage V_{batt} , and $u(t) = [u1, u2]$ corresponds to the power split ratios specified in Section 3.2. The SoC_{final} constraint is the SoC reference for final time $t = t_f$. SoC_{init} is the initial value of the battery SoC at starting time t_0 and can vary between full and empty; if the battery is fully charged the initial value is one (100 %) and if it is empty the initial value is zero (0 %).

The optimal control problem defined by Equation (4.1) depends on the speed profile, $\omega_{whl}(t)$, from which $T_{whl}(t)$ can be computed by using Equation 3.1. If the speed profile is perfectly known a priori; the solution of Equation 4.1 can be found using e.g. dynamic programming. In practice, this is of course never the case.

4.4 Equivalent Consumption Minimization Strategy

The concept of ECMS originates from optimal control theory and can be derived from *Pontryagin's Minimum Principle* [13]. Note that the optimization problem in Equations (4.1)-(3.19) with the SoC constraint removed is a problem of the type

$$J = \min_u \int_{t_0}^{t_f} \mathbf{L}(\mathbf{x}(t), \mathbf{u}(t), t) dt \quad (4.3)$$

subject to

$$\dot{\mathbf{x}}(t) = \mathbf{f}(\mathbf{x}(t), \mathbf{u}(t), t) \quad (4.4)$$

where \mathbf{L} is the so called *Lagrangian*, \mathbf{x} is the system state and \mathbf{u} is the control signal. The cost function should be either minimized or maximized subject to the plant model $\dot{\mathbf{x}}(t)$ and the system constraints. The *Hamiltonian*, \mathcal{H} , can be formulated to be able to solve the optimal control problem. The Hamiltonian is formulated from Equations (4.4) and (4.3), and expressed as

$$\mathcal{H}(\mathbf{x}(t), \mathbf{u}(t), \boldsymbol{\lambda}(t), t) = \mathbf{L}(\mathbf{x}(t), \mathbf{u}(t), t) + \boldsymbol{\lambda}^T(t) \mathbf{f}(\mathbf{x}(t), \mathbf{u}(t), t) \quad (4.5)$$

$$\dot{\boldsymbol{\lambda}}(t) = \frac{-\partial\mathcal{H}(\mathbf{x}, \mathbf{u}, t)}{\partial\mathbf{x}(t)} \quad (4.6)$$

which is subject to minimization (or maximization) with respect to $\mathbf{u}(t)$. The variable $\boldsymbol{\lambda}(t)$ is the *adjoint state*, also called the *Lagrange multiplier* which is an unknown parameter. The optimal control signal is then given by

$$u^* = \min \mathcal{H}(\mathbf{x}(t), \mathbf{u}(t), \boldsymbol{\lambda}(t), t) \quad (4.7)$$

In this thesis the control problem to be solved is to minimize the fuel consumption. Therefore \mathbf{L} is changed to fuel mass flow, \dot{m}_{fuel} , stated in Equation (4.1), and the plant model for this specific problem is $\dot{\mathbf{x}}(t) = \frac{dSOC}{dt}$ as specified in Equation (4.2). If the state dependence is assumed negligible in the state equation, i.e. the voltage is constant in the working area, see Figure 3.8, then the adjoint state, $\boldsymbol{\lambda}$, is constant along the optimal solution [5], [3]. Equation (4.6) is thus reduced to

$$\dot{\lambda}(t) = \frac{-\partial\mathcal{H}(x, u, t)}{\partial x(t)} = 0 \quad (4.8)$$

and the solution is $\lambda(t) = \lambda_0$, where λ_0 is a unknown constant. However, if the trip is unknown a priori, there is no way to determine the correct value of $\lambda(t) = \lambda_0$, which implies that it must be estimated somehow. By exchanging the Lagrangian to the fuel mass flow and using the state equation defined by Equation (4.2), the Hamiltonian can be treated as a cost function according to

$$J = \min_u \left\{ \dot{m}_{fuel} + s(t) \frac{dSoC}{dt} \right\} \quad (4.9)$$

where $s(t)$ is the equivalence factor between electrical energy and fuel energy and is an approximated function of $\lambda(t)$ [3]. The equivalence factor is an approximation since the trip information is not known a priori, which could otherwise provide the true equivalence factor. The main difficulty of ECMS is to approximate a satisfactory equivalence factor.

The equivalence factor The equivalence factor $s(t)$ adjusts the battery energy cost to make it comparable to the fuel energy cost. It is simply stating the answer to “How many units of fuel energy is this unit of stored electric energy worth?” in each time instant. Depending on what information that is available, $s(t)$ may be a function of a number of parameters; current SoC, distance driven and driver demand to name a few. The equivalence factor influences energy management as follows; if $s(t)$ is too large, then the use of electric energy is penalized and the trip is finished with battery charge left, if $s(t)$ is too small, the electric energy is used up too early.

The simplest solution to $s(t)$ is a single, carefully chosen constant $s(t) = s_0$, found based on simulations or trial & error. One way to determine values for a constant equivalence factor, as presented in [4], is to simulate the model with

different power split ratios, performing a sweep over the range of valid power split ratios (defined by Equation (3.17)). The fuel and electric energy use are then summed up for each power split ratio, as in the relation displayed in Figure 4.2. The slopes of the lines are assigned as the constants s_{dis} and s_{chg} , where s_{dis} represents equivalence factor for a net charge of electric energy during the trip while s_{chg} represents a net discharge of the battery during the trip. These constants can be weighed together depending on the amount of expected regenerative braking and trip length, among other things.

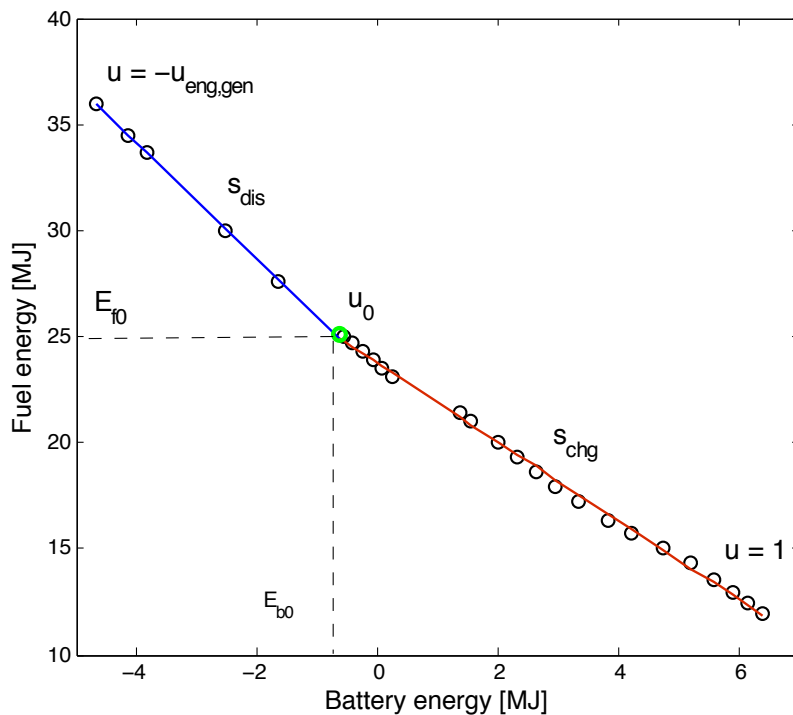


Figure 4.2: Determination of equivalence factors. The parameter u represents the power split between the ICE and the EM. The slopes correspond to suitable charge and discharge "currents".

Using ECMS is beneficial for a number of reasons. Firstly, optimization can be performed offline, by solving the optimization problem and storing the result in lookup tables, allowing operation as a real-time control system [10], [14] and [15]. Secondly, it does not require much modeling of the vehicle besides for ICE and EM efficiencies. Finally, ECMS is easily scaled to how much a priori information there is available (e.g. trip length and road load) by only changing the equivalence factor. It is also easy to follow different discharge strategies such as blended discharge or CDCS, just by changing the SoC reference and the equivalence factor. All of these benefits provide for a structured control system that can easily be inserted to new vehicle models without the need for specific manual tuning of rules and conditions.

5 Implementation of ECMS

The implementation of the ECMS algorithm into the extensive VSim model can be done in a rather simple way since only its energy management subsystem needs to be modified. In short, it is only a matter of a few steps, done in every time instance, that makes the power split decisions based on power demand. Given a power demand, the total cost of propulsion is summed up in a cost function by using lookup tables. This cost calculation model is a subset of the propulsion control system and considers only steady state fuel consumption and electricity losses and not the various states that do take dynamics into account. Note however that once a power split has been calculated and selected by the cost function model, the VSim model and vehicle propulsion control perform simulations with the full functionality it normally has. Prior to calculating the fuel cost and choosing the most efficient power split, the equivalence factor needs to be calculated and weighed into the cost. Its task is to adjust the “price” of electricity usage in order to follow the desired discharge strategy. Below follows a detailed description of how the cost function is calculated and the power split is selected in the ECMS implementation.

5.1 Stating the cost function

In order to minimize the cost of propulsion, in terms of fuel and electricity, a cost function similar to Equation (4.9) is needed to sum up the total energy consumption. However, for use in a simulation environment it is impractical to supervise the battery energy consumption in terms of $\frac{dSoC}{dt}$. Instead it is more convenient to observe the actual electric power drawn from the battery, P_{batt} , which is simple to associate with the consuming electric motor. Similarly, the fuel consumption can be expressed in terms of thermal power as in Equation (3.16). As a result, fuel and electricity consumption can now be compared in quantities of power. Let the cost function from Equation (4.9) be reformulated as

$$J = \min_{(u_1, u_2)} P_{fuel}(t) + s(t)P_{batt}(t) \quad (5.1)$$

where control variables (u_1, u_2) are defined as (3.17) and (3.18) and P_{fuel} according to

$$P_{fuel}(t) = P_{fuel,ICE}(t) + P_{fuel,start}(t) \quad (5.2)$$

where $P_{fuel,ICE}(t)$ is defined by Equation (3.16). The term $P_{start}(t)$ represents an engine start penalty cost that is added every time ECMS requests an engine start. The battery power $P_{batt}(t)$ is given by the total electric power flow from the battery according to

$$P_{batt}(t) = P_{EM,El}(t) + P_{ISG,El}(t) + P_{aux} + P_{batt,loss}(t) \quad (5.3)$$

with $P_{EM,El}$, $P_{ISG,El}$ and $P_{batt,loss}$ given by Equations (3.14), (3.15) and (3.20). The auxiliary power P_{aux} is assumed to be a constant load and is an input from the VSim model. The variable $s(t)$ is the equivalence factor between fuel energy and battery energy consumption.

5.2 Engine startup cost

During the phase of starting the engine, a small but non-negligible quantity of fuel is consumed which implies that the number of engine starts need to be optimized as much as possible. This is the main reason for introducing the penalty cost $P_{start}(t)$ attached to starting the engine. By making the cost vary with speed then not only the number of engine starts can be reduced, they will also occur at more beneficial operating points. This is because it reduces the ability to start the engine and select suboptimal operating points only due to SoC deviation. The general number of starts is reduced by having the cost acting as a threshold between (efficiency-wise) bordering operating points which differ on using the ICE or not. Figures 5.1 and 5.2 illustrate what to consider when it comes to prioritizing efficient operating points with the help of engine start costs as a way of decreasing the negative impact from SoC feedback.

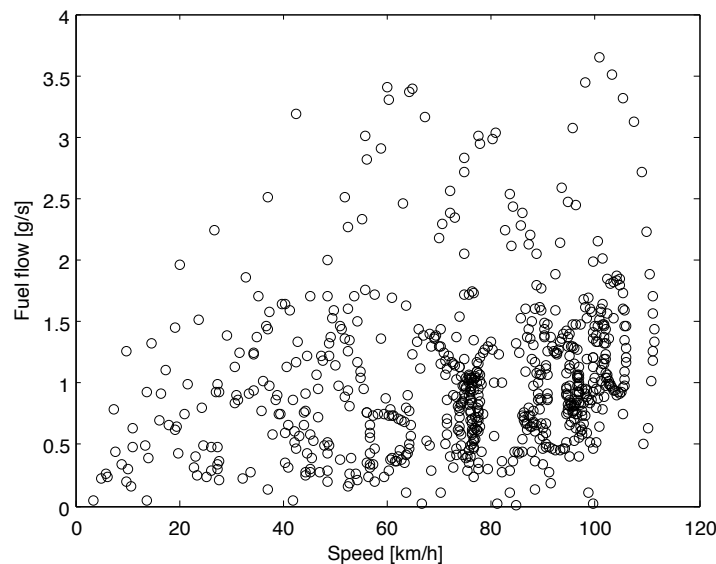


Figure 5.1: Speed and fuel consumption overview of the ICE. Note how similar fuel consumption is for the ICE regardless of high or low speeds. By shifting operating points from the left half plane to the right with the usage of variable engine start costs, a higher efficiency may be reached.

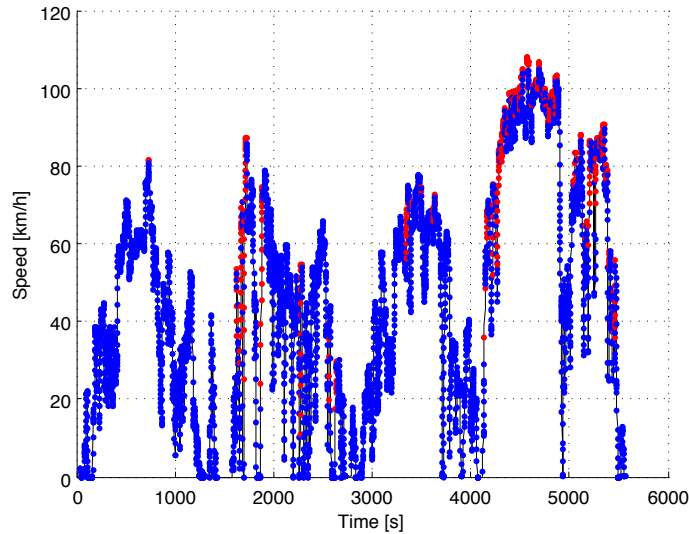


Figure 5.2: An overview of when the ICE (red) and EM (blue) are used in a drive cycle; one dot represents a torque at least twice the torque of the other motor/engine. It would be typically beneficial to not use the ICE on lower speeds. An unfortunate combination of a low speed operating point and a SoC below reference may still lead to such decisions. This is how the speed dependent engine start cost can locally adjust the equivalence factor and generally make an impact on fuel consumption.

By applying the argument concerning the ICE efficiency from Section 3.2.1, a basis for determining the start-up cost of the engine can be established. Given higher efficiency at high vehicle speed, the engine start-up cost should therefore be set lower at such speeds. For the same reason, the cost is set high for low vehicle speeds, a situation where the electric motor instead can operate at a better efficiency. It is important to note that this penalty is not directly determined from the actual physical cost of an engine start. Such a calculation would not be representative to how the cost function evaluates power consumption. The instantaneous power consumption during the start-up process would become very high whereas the actual quantity of consumed fuel is small. Then it is better to implement a perceived startup cost expressed in terms of a smaller fuel power, rendering less of an instant and high threshold.

5.3 Determining the equivalence factor

The equivalence factor $s(t)$ is representing an approximation of the adjoint state $\lambda(t)$, which was assumed constant in the optimal control problem that was described in Section 4.4. If the adjoint state was known, then $s(t) = \lambda(t) = \text{const}$

would by itself suffice for an equivalence factor leading to a satisfactory SoC discharge trajectory. However, since all of the trip information is not known in advance, the equivalence factor has to be approximated. It can be approximated from an average of suitable constants found from earlier simulations, which is denoted by the equivalence constant s_0 . In addition, feedback of the SoC deviation can be used in order to ensure the SoC trajectory to stay close to its reference. The approximated equivalence factor is then given by

$$s(t) = s_0 + s_0 K \tan\left(\frac{SoC_{ref} - SoC(t)}{2\pi}\right) \quad (5.4)$$

which consists of both the adjoint state approximation s_0 as well as a correction based on feedback of deviations from the SoC reference. The feedback of the SoC error is performed by a tangent function, which is a robust and simple way of error elimination, see [16]. Since a tangent function approaches infinity at the limits $\pm\frac{\pi}{2}$, some form of window for SoC deviations needs to be decided within these limits. By scaling the input of the tangent function by $\frac{1}{2\pi}$ and saturating it at the limits $\pm\frac{\pi}{2} \pm 0.1$, the maximum SoC deviation before saturation is found at $\approx 9.8\%$. The factor K is a feedback gain that is used to adjust the amount of feedback given inside the SoC deviation window. This gain changes depending on mode of operation, such as blended mode or sustain mode. In blended mode, K may be relaxed since deviations can still be compensated for. However, when in sustain mode it becomes more important to stay close to the reference, compare the deviation window described above to the CS region displayed in Figure 4.1. An example of the tangent feedback function with different feedback gains can be seen in Figure 5.3.

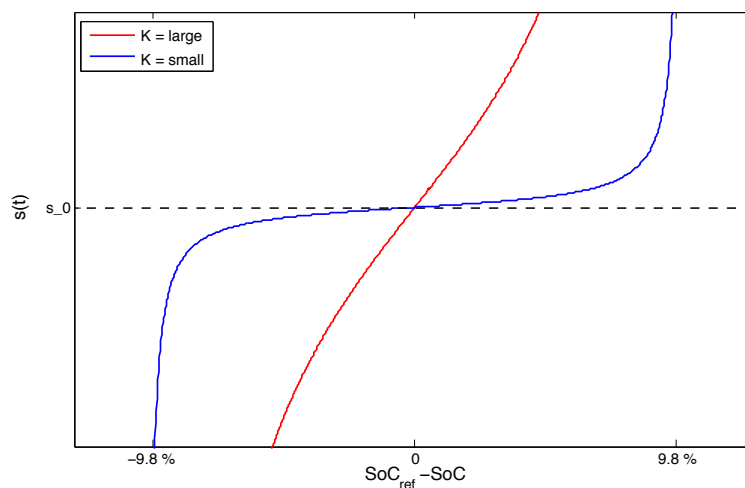


Figure 5.3: The equivalence factor $s(t)$, calculated from Equation (5.4) with two different gains K shown.

Feedback of the SoC reference is used because at least some sort of correction is necessary since the optimal s_0 can only be estimated and not found due to lack of future trip information. The SoC reference is defined with the background of related works [3], [15], suggesting that an optimal SoC trajectory is typically decreasing linearly with distance covered $d(t)$:

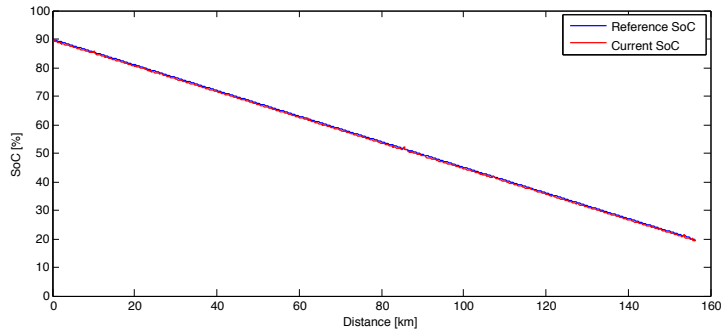
$$SoC_{ref}(t) = \frac{(SoC_{final} - SoC_{init})}{D_{tot}}d(t) + SoC_{init} \quad (5.5)$$

A small but important detail when it comes to estimation of the total trip distance, D_{tot} , for use in a blended mode strategy is related to estimation errors. If the total trip length turns out to be shorter than expected, then there will be a remaining amount of SoC in the battery. This consequently leads to more fuel consumed than was necessary assuming the battery will be recharged after the trip. For this reason it is good to underestimate the trip length slightly, since operating in CS mode for the last bit does not bring the same losses. For the same reason, the simulations were conducted with slightly underestimated trip lengths, even if the exact distances were known. The trip distances were estimated by multiplying the average speed with the total time of each drive cycle, rounded down to nearest integer (kilometer).

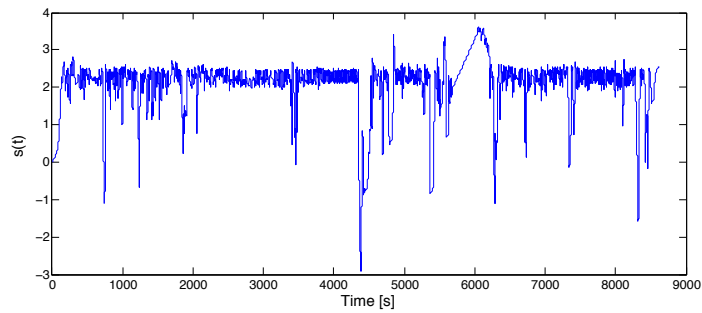
The equivalence constant is derived based on the notion that for a given drive cycle, a typically desirable SoC trajectory (linearly decreasing over distance) with $s(t)$ as its only control input will also provide a corresponding suitable equivalence constant. An approximation for s_0 for the corresponding drive cycle can be determined in a single simulation run while using a large gain proportional feedback, P , of the SoC error which keeps the SoC deviations small:

$$s(t) = P(SoC_{ref} - SoC(t)) \quad (5.6)$$

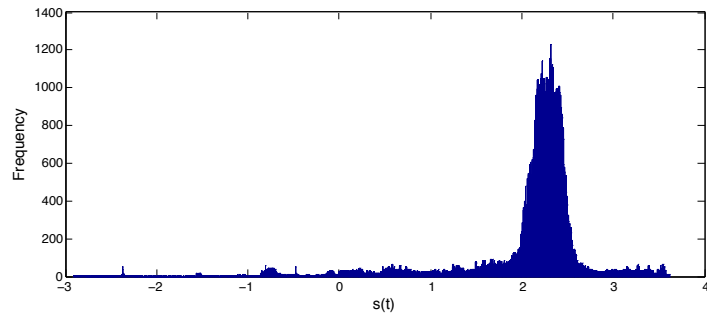
The equivalence constant is then presented as the mean of $s(t)$ for that drive cycle. Assuming that a blended discharge mode according to Figure 4.1 is desired for a given drive cycle and between two specified SoC limits, the corresponding equivalence constant s_0 can then be determined according to Figure 5.4.



(a) SoC trajectory in relation to the SoC reference. Deviations are fed back with a large proportional gain which associates $s(t)$ with the history of the corresponding reference following SoC trajectory.



(b) The $s(t)$ is turbulent with a large gain P-controller, ensuring close reference tracking



(c) The mean of $s(t)$ suggests a suitable value for s_0 . If the ability to discharge is not saturated then $s(t)$ will stay close to the desired SoC trajectory most of the time. As a consequence, the mean of $s(t)$ provides an s_0 that follows said trajectory on average, resulting in a coarse blended mode discharge by itself.

Figure 5.4: A method of determining s_0 in a single simulation run, given a drive cycle and limits for initial and final SoC.

If a sustaining behavior is desired, for example when SoC is low and CS mode must be engaged, an equivalence constant $s_{sustain}$ needs to be determined and used. The method illustrated in Figure 4.2 can be used to generate a sustaining equivalence constant according to

$$s_{sustain} \approx \frac{s_{chg} + s_{dis}}{2} \quad (5.7)$$

Now there are two equivalence constants for the sustain mode and the blended mode, see Figure 5.5. As a reference, all the equivalence constants are related so that

$$s_{chg} \leq s_0 \leq s_{sustain} < s_{dis} \quad (5.8)$$

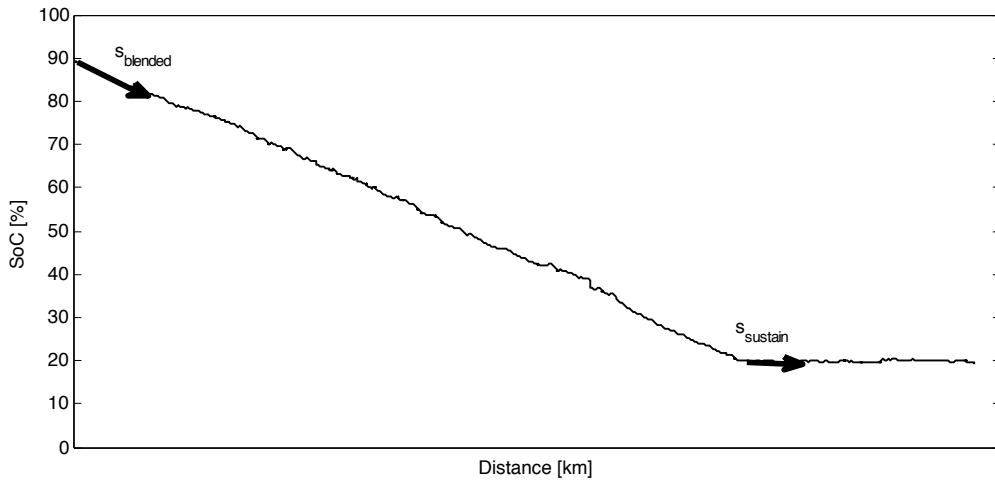


Figure 5.5: The two equivalence constants for blended mode and sustain mode respectively. Setting s_0 in Equation (5.4) equal to one of them makes the SoC discharge trajectory more prone to follow the associated behavior.

It should be pointed out that ECMS allows for other discharge strategies than blended mode. If a CDCS strategy is desired then it is simple enough to directly set the SoC reference to the final SoC level and then schedule a change of s_0 and K for the CS mode once the SoC limit has been reached.

5.4 Implementing the ECMS algorithm

The implementation of ECMS in VSim is realized by a MATLAB embedded function block. This block has the entire algorithm inside including function calls for lookup tables needed to process the cost function calculation. The necessary inputs are routed into the function block from various subsystems of the vehicle model; a complete list of the used input parameters can be viewed in Appendix B. This list may seem long for real-time operation, but the ECMS algorithm can be narrowed down to a “black box” model consisting of lookup tables with pre-calculated values with three input parameters; $T_{whl}(t)$, $\omega_{whl}(t)$ and $s(t)$. What has to be determined off-line though, is the scheduled values ($s_{blended}$, $s_{sustain}$) for the equivalence constant s_0 to be used in the calculation of $s(t)$ and the feedback gain K . The implemented ECMS algorithm is presented as pseudo code in Algorithm 1. Figure 5.6 shows a brief overview of the states used in the ECMS implementation in the VSim model. The ECMS block has (partially) replaced the energy management block from Figure 3.1.

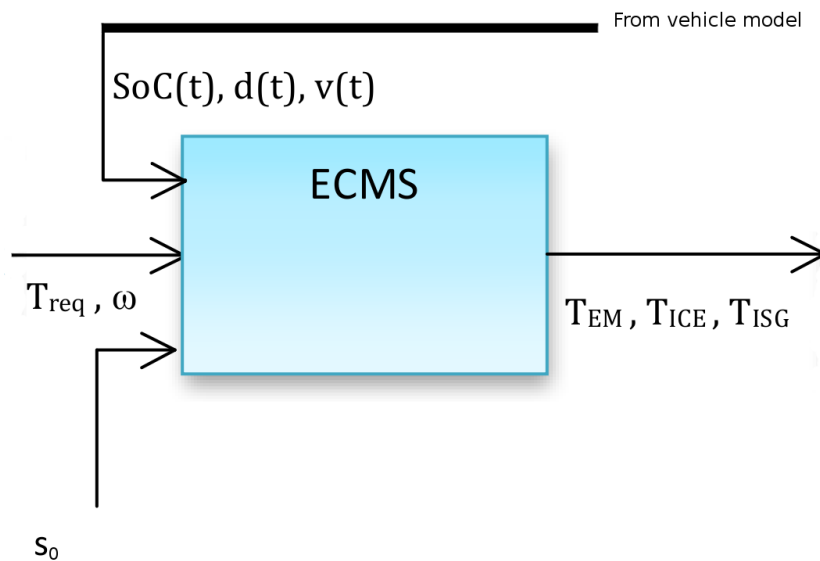


Figure 5.6: A flowchart of the ECMS implementation showing the input and output states needed for the algorithm.

Algorithm 1 Pseudocode for the ECMS algorithm

```
procedure ECMS( $SoC, d, T_{whl}, \omega_{whl}, gr_{GB}, V_{batt}$ ) ▷ Input
  for  $u_1 = [0, \dots, 1]$  do
    for  $u_2 = [u_{2,min}, \dots, u_{2,max}]$  do
       $P_{batt} = P_{EM,El} + P_{aux} + P_{ISG,El} + P_{batt,loss}$ 
      if ICE off then ▷ Check engine status
         $P_{fuel,start} \leftarrow f(\omega_{whl})$ 
         $P_{fuel} = P_{fuel,ICE} + P_{fuel,start}$ 
      else
         $P_{fuel} = P_{fuel,ICE}$ 
      end if
    end for
  end for
  if  $SoC > SoC_{final}$  AND  $d < D_{tot}$  then ▷ Check constraints
     $K \leftarrow K_{blended}$ 
     $s_0 \leftarrow s_{blended}$ 
     $SoC_{ref} = \frac{(SoC_{final} - SoC_{init})}{D_{tot}} d + SoC_{init}$ 
  else
     $K \leftarrow K_{sustain}$ 
     $s_0 \leftarrow s_{sustain}$ 
     $SoC_{ref} = SoC_{final}$ 
  end if
   $\Delta SoC = \frac{SoC_{ref} - SoC}{2\pi}$ 
   $s(t) = s_0 + s_0 K \tan(\Delta SoC)$ 
   $J = P_{fuel} + s(t) P_{batt}$ 
   $\{u_1, u_2\} \leftarrow \min(J)$ 
   $T_{EM} = T_{whl} u_1$  ▷ Output
   $T_{ICE} = T_{whl} (1 - u_1) (1 - u_2)$ 
   $T_{ISG} = T_{whl} (1 - u_1) u_2$ 
end procedure
```

6 Results

In this section the results from simulations of the ECMS control strategy and the nominal control strategy will be presented and an analysis and discussion of the result will be done in Sections 7 and 8. The different drive cycles used to evaluate the ECMS are presented in Appendix A where the trips are referred to as in order of appearance. For all the drive cycles used, the trip length is longer than the AER, ~ 50 km. The simulated drive cycles have a trip length between 60 km to 150 km. First the calculation of the equivalence factor is presented, for both the blended case and the sustain case, see Section 5. Then the resulting values of the engine start cost P_{start} are presented. The majority of the chapter is then dedicated to the evaluation of the ECMS performance with respect to fuel consumption and battery losses. The evaluation is made by comparing the results from a CDCS discharge strategy that has been followed by both the ECMS and the rule-based control strategies. Finally the results of the blended mode strategy under ECMS control are displayed in comparison to the rule-based CDCS strategy, first side-by-side as a table but also in the form of an extended presentation of drive cycles, discharge trajectories, torque distribution and cycled battery current. Every drive cycle is presented separately and in connection with its corresponding figures.

6.1 Equivalence factor

To select s_0 , the vehicle model was simulated with Trips number 4, 7 and 8. The initial and final values for the SoC trajectory are specified in Table 6.1.

Table 6.1: Parameters for calculation of s_0 in blended mode.

| Constant | Value |
|---------------|-------|
| SoC_{init} | 90% |
| SoC_{final} | 20% |

The equivalence factor was calculated according to the methods presented in Section 5.3. When determining $s_{blended}$, Equation (5.6) was used and the value of the gain, P , was selected to 5, allowing close reference tracking. This resulted in the values for $s_{blended}$ as presented in Table 6.2. The average of $s_{blended}$ is then used for the constant s_0 during blended mode discharge.

Table 6.2: s_0 for three different drive cycles.

| Drive cycle | Trip 4 | Trip 7 | Trip 8 | Average value |
|-------------|--------------|-------------------|-------------------|---------------|
| Length | 156 km | 60 km | 120 km | |
| Type | logged mixed | synthetic highway | synthetic highway | |
| s_0 | 2.0748 | 1.98 | 2.0753 | 2.04 |

The calculation of $s_{sustain}$ was made according to Equation (5.7) and the method shown in Figure 4.2, by performing a sweep in the New European Drive Cycle (NEDC), which has a driving distance of 10.9 km. With the values for $s_{dis} = 2.75$ and $s_{chg} = 1.85$, the sustaining equivalence constant was then set as $s_{sustain} = 2.3$. The tangent function slope K had to be simulated iteratively to find suitable values for the blended and sustaining modes. In Table 6.3 a summary of the values found for s_0 and K is presented. The trajectories of $s(t)$ for the different drive cycles can be seen in Appendix C.

Table 6.3: The resulting values for the equivalence factor.

| Constant | Blended mode | sustain mode |
|----------|--------------|--------------|
| s_0 | 2.04 | 2.3 |
| K | 0.5 | 10 |

6.2 Start penalty

In order to avoid inefficient ICE operating points, the concept of engine start costs varying with speed was introduced, as discussed in Section 5. The variable for adjusting the engine start penalty, P_{start} , was chosen to have four different values according to four different vehicle speed intervals. The speed intervals and values for P_{start} were selected empirically from a small number of simulation trials with drive cycles shown in Figures A.2 and A.6. The engine penalty costs and speed intervals found are specified as

$$P_{start} = \begin{cases} 20 \text{ kW} & \text{if } v < 40 \text{ km/h} \\ 17 \text{ kW} & \text{if } 40 \text{ km/h} < v < 50 \text{ km/h} \\ 15 \text{ kW} & \text{if } 50 \text{ km/h} < v < 80 \text{ km/h} \\ 6 \text{ kW} & \text{if } v > 80 \text{ km/h} \end{cases}$$

In Figure 6.1 the speed profile is shown for Trip 1. In the figure it is possible to see that the EM is used in the regions of low speed and the ICE used at high

speed or when the acceleration is large. One exception is at the end of the trip when either the estimated range or the SoC target has been reached before the actual trip is finished. In Figure 6.2 the corresponding fuel consumption can be seen.

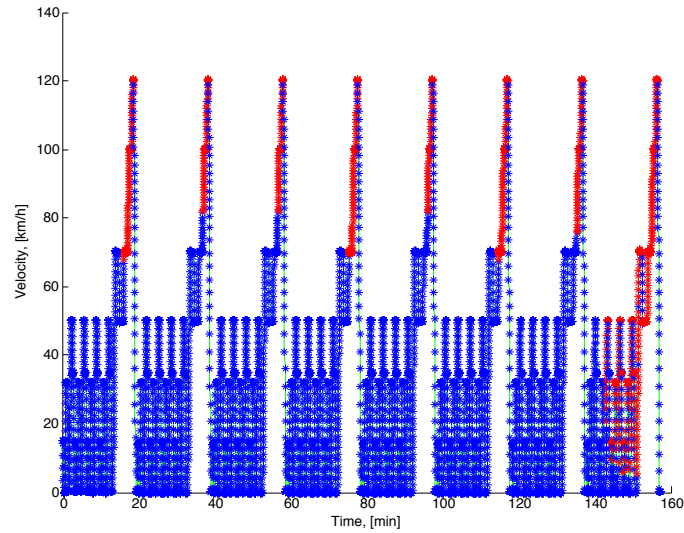


Figure 6.1: The blue dots correspond to at least *twice* as much power usage from the EM compared to the ICE, and vice versa for the red dots. It can be seen that the ICE is only used at high speeds, except from the end, where either the SoC target or estimated distance has been reached.

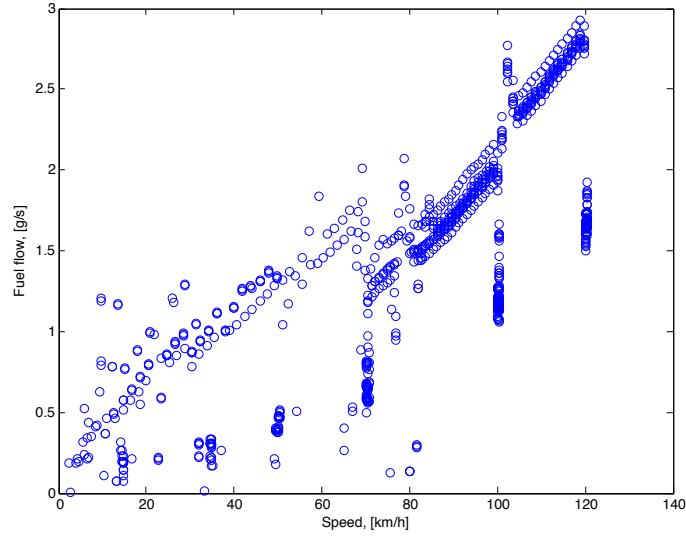


Figure 6.2: The fuel consumption for 8 NEDC. At the end the ICE is used, therefore there is some consumed fuel at the low speeds as well. This is something to be avoided and with a better estimation of the total drive distance it might be possible.

6.3 ECMS performance

In the evaluation of the ECMS performance, the use of the ISG for power split calculations is not included, due to the long simulation time as a result of the complex model. This means that $u_2 = 0$ for all of the results, i.e. the ISG is idle. A range of different values of u_1 are used for calculations when minimizing the cost function J . The power split ratios used are: $u_1 = [0, 0.1, \dots, 0.9, 1]$. This means that size of the cost function grid is 10×1 , and by searching for the minimum value in this grid it is possible to extract the power split that caused the minimum.

The results presented include the relative fuel consumption, the Root Mean Square (RMS) current (i_{RMS}), the average power loss ($\bar{P}_{batt,loss}$) in the battery and the battery Ah-throughput (Ah_{batt}). They are presented in relation to the nominal result according to

$$result = \frac{result_{ECMS}}{result_{nominal}} \quad (6.1)$$

This means that if the percentage are lower than 100 % then ECMS performs a reduction and if the result is higher than 100 % the ECMS solution makes an increase. The battery current, i_{RMS} , used for comparison is calculated as

$$i_{RMS} = \sqrt{\frac{1}{N} \sum_{k=0}^N i_k^2} \quad (6.2)$$

where i is the battery current, see Figure 3.7, and N is the number of samples. The average battery power loss, $P_{batt,loss,avg}$, is calculated based on the mean value of the battery resistance R_{batt} that can vary slightly during the drive.

$$\bar{P}_{batt,loss} = R_{batt} i_{rms}^2 \quad (6.3)$$

The battery Ah-throughput is calculated based on the battery current as

$$Ah_{batt} = \frac{1}{3600} \int_0^{t_f} |i(t)| dt \quad (6.4)$$

The final SoC deviation, ΔSoC_{end} between the two control strategies is calculated as

$$\Delta SoC_{end} = SoC_{final,ECMS} - SoC_{final,nom} \quad (6.5)$$

and based in this deviation from the target SoC at 20 % a fuel correction can be done. The fuel correction is calculated based on the mean value of the equivalence factor $s(t)$, \bar{s} , the battery current throughput and the battery voltage at the end as specified in Equation (6.6). This value is then subtracted from the fuel consumption taken from the simulation results.

$$m_{fuel,corr} = m_{fuel} - \bar{s} \frac{3600 Ah_{batt} V_{batt,end}}{Q_{lhv}} \Delta SoC_{end} \quad (6.6)$$

The results from the two control strategies are presented, in relation to each other, according to Equation (6.1), in Table 6.4. ECMS is performed with both of the two discharge strategies, blended and CDCS.

For Trip 1, Trip 2 and Trip 4 the accumulated battery losses are also calculated and presented in figures. For comparison the results are presented in normalized units, as in Equation (6.1). The accumulated battery losses is calculated based on the battery current, i , and the battery resistance, R_{batt} as

$$W(t) = \int_0^t R_{batt}(\tau) i(\tau)^2 d\tau \quad (6.7)$$

The battery resistance is varying during the drive cycle and therefore it is also included in the integral.

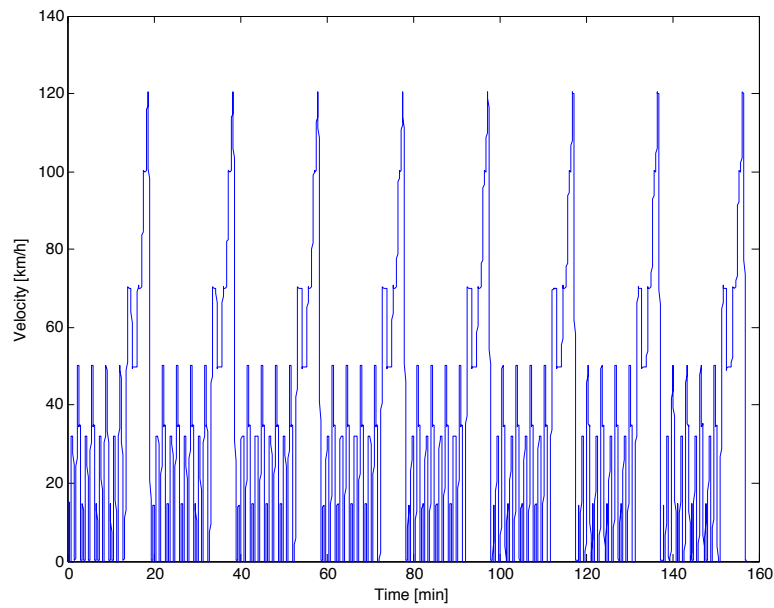
For Trip 1 the drive profile and a cutout of the torque applied on the wheels are presented in Figure 6.3, the SoC profile for ECMS using the blended mode discharge and the nominal control strategy with the CDCS mode discharge are presented in Figure 6.4. It can be noticed that the SoC reaches the final SoC, 20 %, before the trip is finished. The trip length for this drive cycle is estimated to 80 km, it was assumed that one NEDC part is ~ 10 km, but the travel distance is 87.2 km. In Figure 6.5 the accumulated battery losses is presented.

Table 6.4: The ECMS performance for blended mode discharge *and* for CDCS mode discharge in relation to the nominal, rule-based control strategy with CDCS discharge.

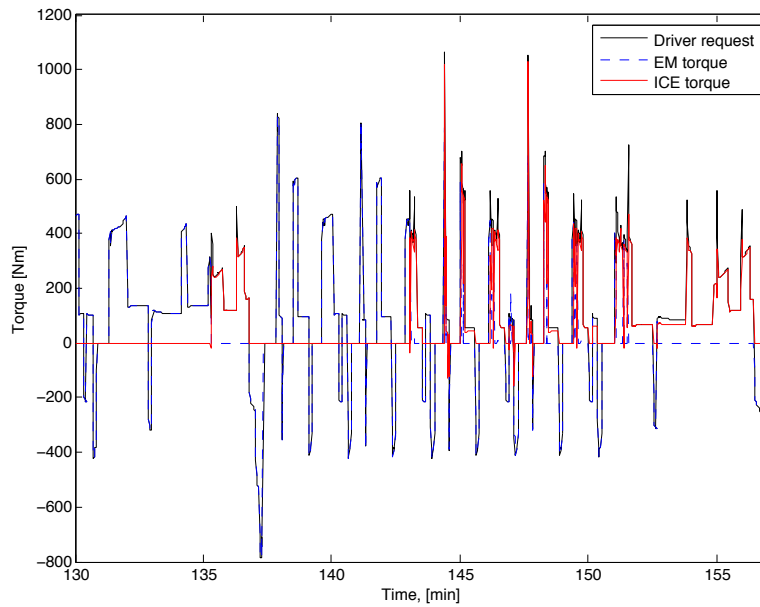
| Trip (length) | Discharge | m_{fuel} | $m_{fuel,corr}$ | i_{RMS} | $P_{batt,loss}$ | Ah_{batt} | ΔSoC_{end} |
|-----------------------------------|-----------|------------|-----------------|-----------|-----------------|-------------|--------------------|
| 1 (~ 80 km) 8 x NEDC | Blended | 93.5 % | 95.2 % | 85.2 % | 72.0 % | 82.0 % | -2.3 % |
| | CDCS | 101.2 % | 101.2 % | 95.7 % | 92.1 % | 82.2 % | -1.6 % |
| 2 (~ 67 km) logged mixed | Blended | 96.3 % | 96.6 % | 98.8 % | 98.1 % | 98.4 % | -0.2 % |
| | CDCS | 96.7 % | 95.5 % | 99.3 % | 98.6 % | 98.4 % | -0.3 % |
| 3 (~ 67 km) logged mixed | Blended | 91.0 % | 88.0 % | 91.4 % | 82.2 % | 88.8 % | 1.5 % |
| | CDCS | 97.9 % | 97.8 % | 96.9 % | 93.6 % | 90.4 % | 0.3 % |
| 4 (~ 156 km) logged mixed | Blended | 98.5 % | 98.7 % | 86.9 % | 75.6 % | 79.6 % | -1.1 % |
| | CDCS | 97.6 % | 100.5 % | 92.1 % | 84.1 % | 86.0 % | -5.7 % |
| 5 (~ 92 km) logged freeway | Blended | 95.2 % | 95.5 % | 99.0 % | 100.0 % | 97.5 % | -0.4 % |
| | CDCS | 97.8 % | 97.6 % | 99.7 % | 99.4 % | 98.2 % | -0.4 % |
| 6 (~ 92 km) logged mixed | Blended | 99.6 % | 100.0 % | 84.8 % | 71.0 % | 80.9 % | -0.6 % |
| | CDCS | 103.9 % | 104.3 % | 92.1 % | 84.6 % | 83.4 % | -1.0 % |
| 8 (~ 120 km) synthetic freeway | Blended | 96.4 % | 96.5 % | 94.6 % | 91.9 % | 96.6 % | -0.5 % |
| | CDCS | 93.0 % | 96.0 % | 100.3 % | 100.4 % | 100.9 % | -4.3 % |

Trip 2 drive profile and a cutout of the torque requested and applied on the front and rear wheels are presented in Figure 6.6. Note that the cutout of the torque is at the high speed part in the drive profile, meaning that the penalty for an ICE start is low. For this trip the estimated driving distance is 67 km and the total driving distance is 67.94 km. The SoC trajectory is presented in Figure 6.7 and the accumulated battery losses in the battery is presented in Figure 6.8

The drive profile for Trip 4 is shown in Figure 6.9. This drive cycle is estimated to have a trip length of 156 km, the true length is 156.39 km and this is the drive cycle with the longest distance. A cutout of the the requested EM and ICE torques can be seen in Figure 6.9. The SoC trajectory is presented in Figure 6.10 and the accumulated battery losses is presented in Figure 6.11.



(a) Drive profile for Trip 1, the NEDC repeated 8 times.



(b) A cutout of the torque requested from the driver and the delivered wheel torque for both front wheel and rear wheel.

Figure 6.3: The performance for 8 NEDC, Trip 1. The driver profile and the torque for EM and ICE is presented, the estimated trip length is 80 km but in reality it is 87.2 km.

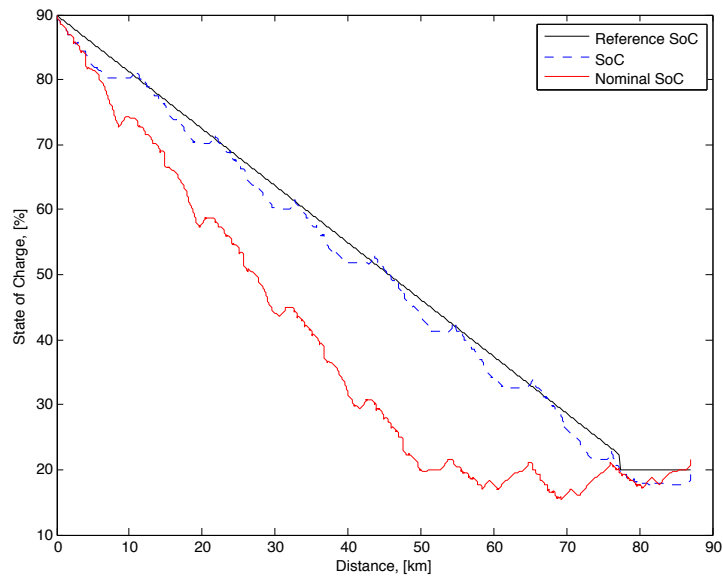


Figure 6.4: The SoC trajectories for both the ECMS with blended discharge and the nominal control strategy the CDCS strategy for Trip 1.

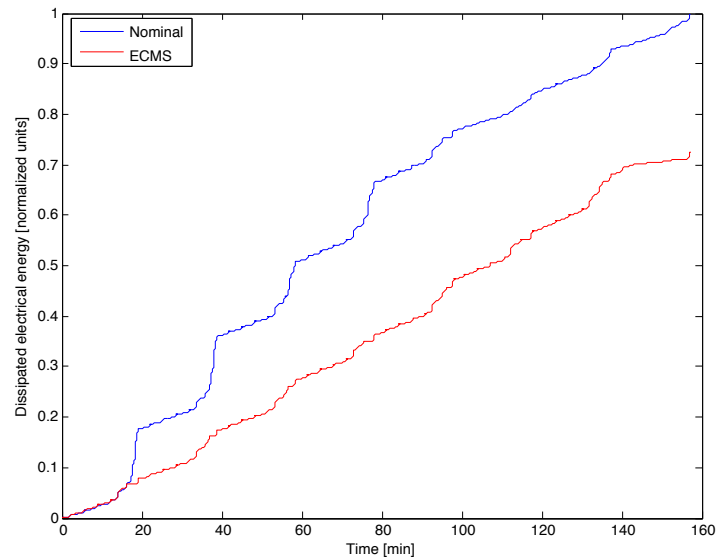
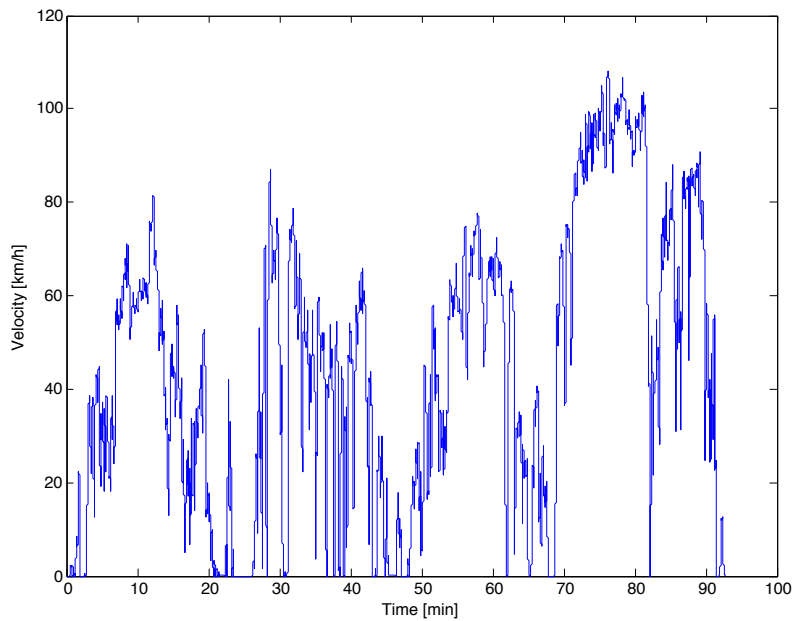
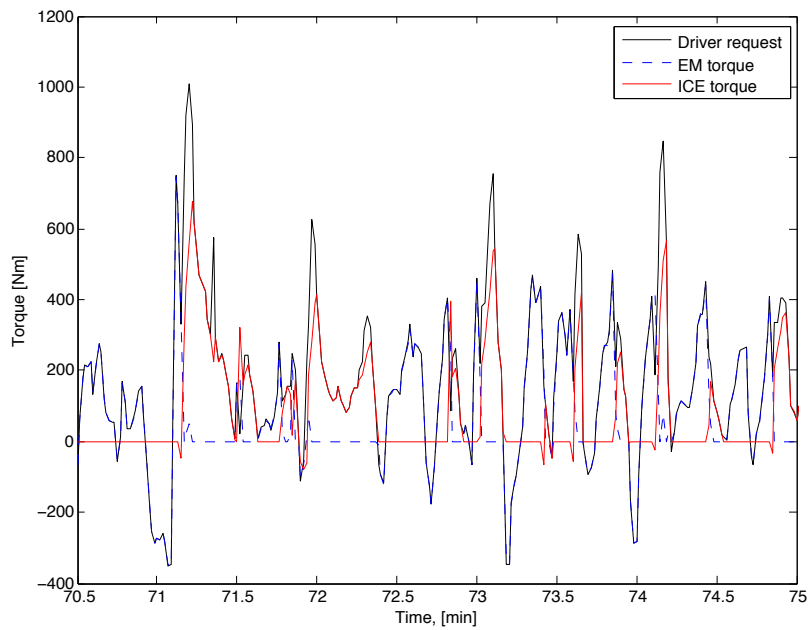


Figure 6.5: The accumulated battery losses Trip 1. The result is presented in normalized units, the ECMS, with blended discharge, is $\sim 30\%$ better.



(a) Drive profile for Trip 2.



(b) A cutout of the torque requested from the driver and the delivered wheel torque for both front wheel and rear wheel. Note that this is in the high speed part.

Figure 6.6: The performance for Trip 2. The driver profile and a cutout of the requested torque and the torque for the EM and the ICE is presented. The estimated trip length is 67 km but in reality it is 67.94 km.

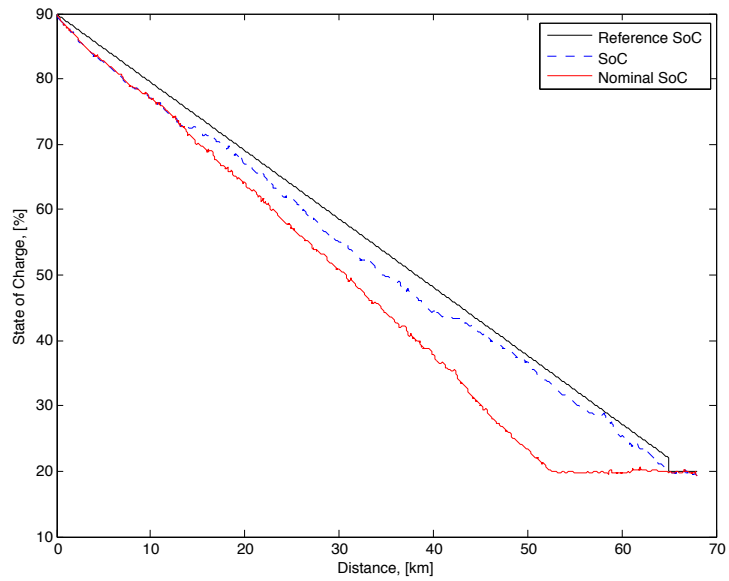


Figure 6.7: The SoC trajectories for Trip 2 for both the ECMS with blended discharge and the nominal, rule-based CDCS strategy.

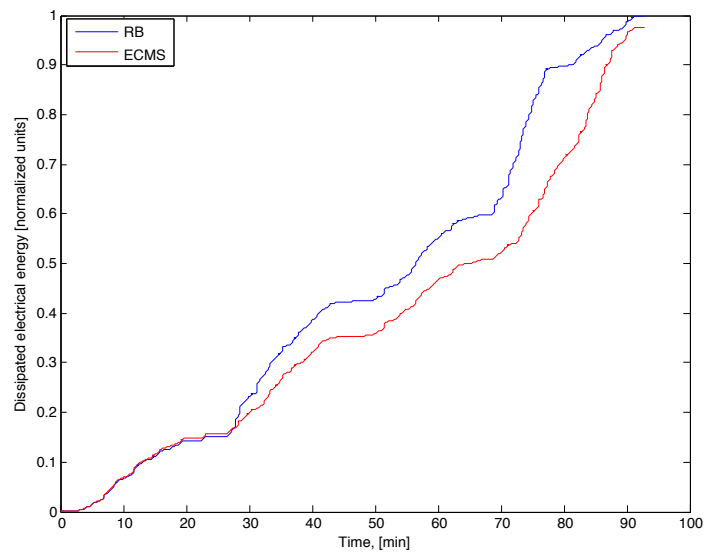
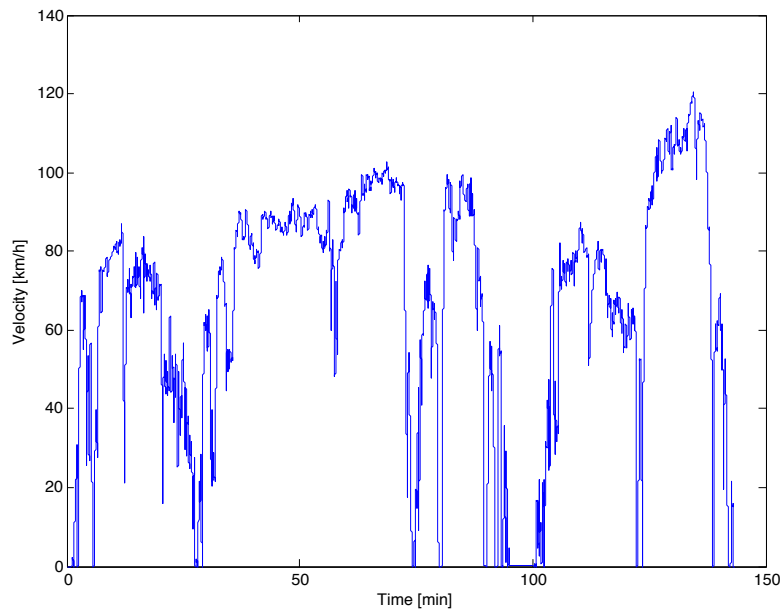
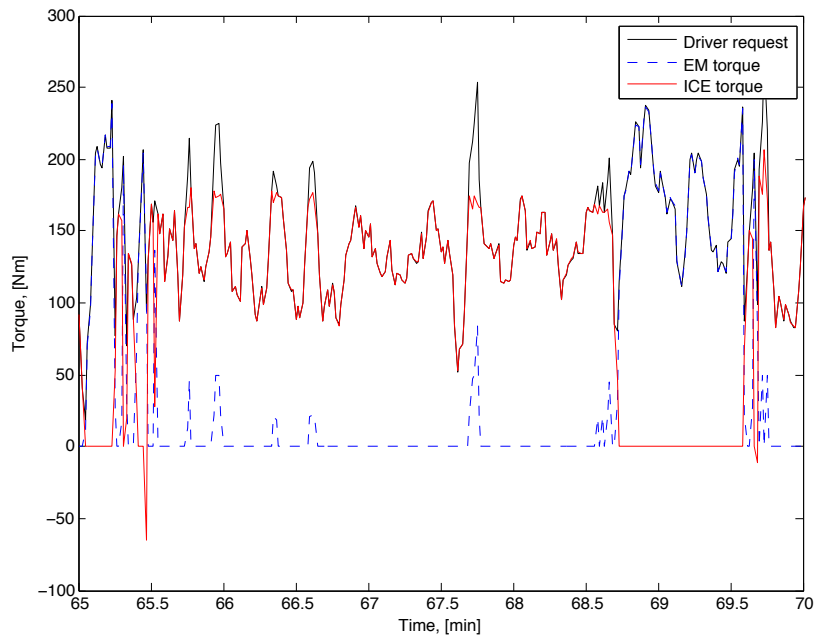


Figure 6.8: The accumulated battery losses for Trip 2. The result is presented in normalized units, the ECMS, with blended discharge, is $\sim 5\%$ better.



(a) Drive profile for Trip 4s.



(b) A cutout of the torque requested from the driver and the delivered wheel torque for both front wheel and rear wheel.

Figure 6.9: The performance for Trip 4. The driver profile and a cutout of the torque. The estimated trip length is 156 km the true distance is 156.39 km.

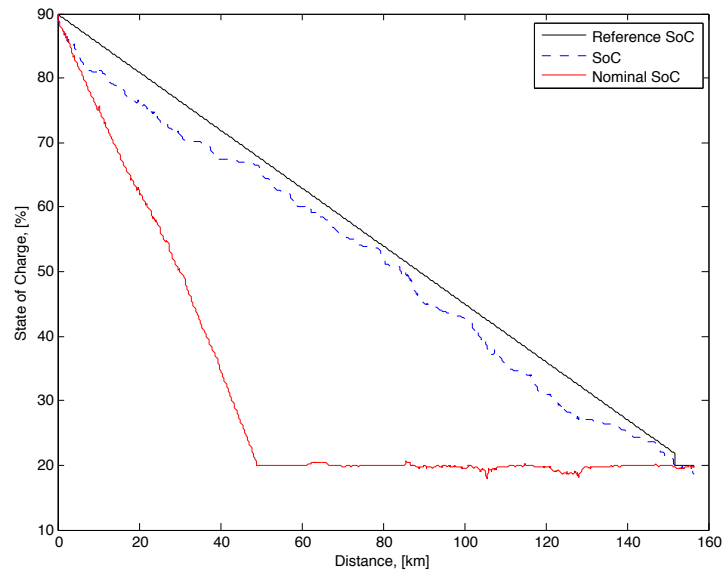


Figure 6.10: The SoC trajectories for Trip 4 for both the ECMS with blended discharge and the nominal, rule-based CDCS strategy.

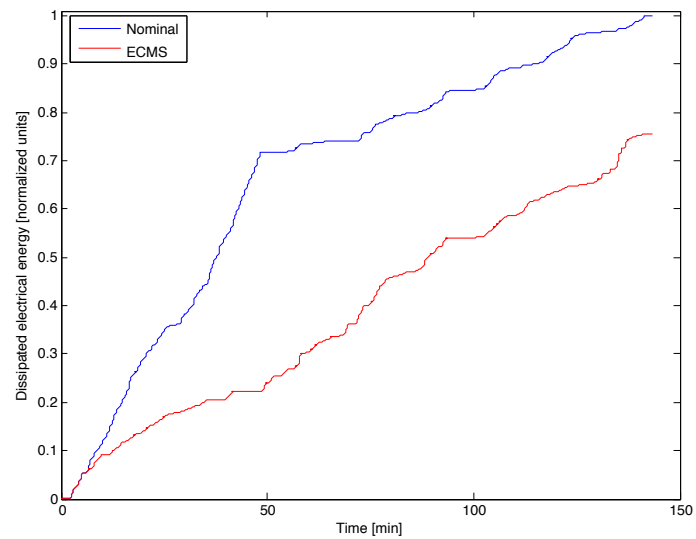


Figure 6.11: The accumulated battery losses for Trip 4. The result is presented in normalized units, the ECMS, with blended discharge, is $\sim 30\%$ better.

7 Analysis

In the following section, an analysis of the respective results is presented.

7.1 Fuel consumption

The results in Table 6.4 are indicating that the ECMS strategy perform better for all of the 8 drive cycles evaluated, reducing the fuel consumption in the range of 1 – 9 % and by 4.2 % on average. These figures are presented without considering the difference in SoC at the end of the trip between the two strategies compared. A correction would be to multiply the remaining energy quantity by the average of the equivalence factor (as a measure of efficiency), according to Equation (6.6). The reduction in fuel consumption would then span between 0 – 12 % but the average remains at 4.2 %. Note that this is an estimation of the corrected fuel consumption, the true efficiency of the supposed engine operation remains unknown.

It can be noted that the fuel consumption for ECMS with CDCS is also reduced but not so much as for the blended discharge strategy. The change varied from +3 % to –7 % (uncorrected) but yet made a 1.7 % reduction on average, the corrected average is 1.0 %. For Trip 1, while using CDCS, the fuel consumption increased, possibly because the nominal controller is tuned specifically towards this drive cycle while the ECMS algorithm is tuned completely towards a blended mode discharge. The parameters s_0 , K and P_{start} can be modified for such tuning.

7.2 Engine start cost

The introduction of the perceived engine start cost, P_{start} , made a significant difference in reducing the number of engine starts. Further tuning of P_{start} consisting of varying the start cost for different vehicle speed intervals contributed to a large impact in fuel consumption, resulting in a relative reduction for blended mode discharge for all of the 8 drive cycles that were evaluated. The main advantage that a variable engine start cost brings, besides reducing the number of engine starts, is also the ability to prioritize the decision to select the power split based on *efficiency* rather than selection due to temporary *SoC deviation*. This can be described as to locally adjust the SoC reference up or down slightly to override the SoC feedback functionality for a certain SoC deviation, based on information known externally (e.g. electric propulsion is preferred at low speed).

7.3 Battery operation

Evaluation of battery operation in terms of battery life can be done with respect to a number of parameters [11], of which a few of them are analyzed here. The results presented in Table 6.4 show comparisons of RMS current, battery power losses and total current throughput. Another parameter that affects battery life is the time spent at low SoC levels, which can be observed from the SoC discharge trajectories displayed in figures from Section 6.3. All results are analyzed with respect to the ECMS control strategy in relation to the nominal rule-based strategy with a CDCS discharge strategy.

Starting with the battery RMS currents, i_{RMS} , which were found to be reduced, on average, by 8.5 % for blended mode and 3.4 % for the ECMS using the CDCS strategy. The resulting battery power losses, $P_{batt,loss,avg}$, were on average reduced by 15.6 % in blended mode and 6.7 % for CDCS. Reductions in blended mode driving is an expected consequence from the ability of the EM to operate at lower current levels by avoiding suboptimal operating points, as higher currents induce more losses, according to Equation (6.3). As a side note, it may be expected that power losses would be proportional to the square of the RMS currents. The reason of why the results show a slight deviation in this regard is because the battery resistances were not identical between the two cases, which is why it does not add up. Another important reason for the power loss reduction is the higher average battery voltage at which the EM operates at during blended mode, despite being used frequently, which lowers the necessary current for a specific power according to $P = UI$.

Additionally, the total electric energy cycled through the battery, Ah_{batt} , was also found lower for both discharge strategies. Blended mode resulted in a 10.9 % reduction on average and CDCS made a 8.6 % reduction. This is illustrated in Figures 6.5, 6.8 and 6.11. The reductions presented above are all contributors to maintaining a long battery life, as well as the shorter time spent at low SoC levels which has only been presented in figures.

7.4 Drive cycle influence

By comparing the fuel consumption results in Table 6.4 for Trips 2 and 3, it can be noted that there is a difference in consumption between the ECMS controlled strategies compared to the rule-based case. It is notable because the only difference is within the order of two different speed segments. Trip 2, see Figure A.2, begins with a low speed segment and ends with a high speed segment. However, Trip 3, see Figure A.3, begins with the same high speed part of Trip 2 and ends with the low speed part of Trip 2. The fact that the nominal strategy varies significantly in fuel consumption compared to ECMS despite that the same drive cycles are used suggests that the CDCS discharge strategy is quite sensitive to such “unfortunate” drive cycle designs. The ECMS control strategy with blended discharge could then be considered more robust to such variation in drive cycle design.

When looking at whether high or low speeds in general influence one strategy or

the other, some small indications can be observed. The rule-based control strategy with CDCS performs its best, close to ECMS, for drive cycles with more low speed segments, for example Trip 6. When it comes to high speed segments, for example Trip 5, ECMS for both discharge strategies perform significantly better ($\sim 4\%$) than the rule-based control strategy with CDCS.

7.5 Equivalence factor

The method used to determine the equivalence constant $s_{blended}$ in Section 5.3 has been found to provide suitable constants for blended mode operation, resulting in satisfactory SoC trajectories without using too much SoC feedback. It is also efficient as it only requires a single run per drive cycle. For the ECMS control under the CDCS discharge strategy, the equivalence constant s_0 used during depletion was the same as for blended mode discharge. If the equivalence constant would have been tuned specifically (slightly lower) for this discharge strategy instead (during CD mode), the results might have differed slightly in favor to ECMS.

The sustain constant $s_{sustain}$ was found based on the method of sweeping different power split ratios and evaluating the energy for each of them. This value was only based on one simulation with the NEDC drive cycle, which is shorter than the AER. The variation of $s(t)$, seen in Appendix C, at the end is quite high, this is mainly due to the slope of the tangent function, which is higher in sustaining mode, i.e. when the estimated distance D_{tot} has been exceeded or if the SoC target has been reached. During normal operation, $s(t)$ does not exceed the limits but it may show some variation.

8 Discussion

The results are in general satisfactory and to some extent also expected. However, there are some aspects that were not clear after the analysis and need further discussion.

8.1 Reducing the fuel consumption

The blended mode discharge strategy operating under ECMS has shown a reduction in fuel consumption. This is possible mainly thanks to a more selective use of the EM and ICE by matching them to suitable operating points. Such matching leads to increased fuel efficiency as well as lowered electric power losses. Another contributing factor is the engine start penalty cost which helped reducing the number of engine starts as well as locally reducing the influence of the SoC dependence, avoiding suboptimal operating points.

It can be seen though, that fuel consumption was not reduced for all cases investigated. Some particular drive cycles resulted in increased fuel consumption for the CDCS strategy under ECMS control. This might depend on the fact that the ECMS algorithm was not at all tuned for the CDCS case. If some tuning of both s_0 and P_{start} were to be made, the results might turn out differently. Additionally, the nominal strategy uses the ISG at some points while it is not used at all in the ECMS control algorithm studied in this thesis. This can possibly be what is influencing the results. The use of the ISG may lead to either higher or lower fuel consumption for the ECMS control strategy depending on how well it is utilized. The utilization of the ISG might as well explain why the nominal CDCS alternative is better sometimes and sometimes not.

8.2 Battery life

The stress of the battery was lowered when using the ECMS algorithm to solve the control problem, for both blended and CDCS battery discharge. This is an advantage because, if the battery losses are higher, the battery will need more cooling which means that more auxiliary power has to be used for battery cooling. Indirectly, this will eventually lead to increasing fuel consumption due to the extra amount of battery energy consumed for the auxiliary power demanded. In the vehicle model used, the cooling power is not modeled and temperature effects are therefore not taken into account. The battery losses are lower with the ECMS algorithm which would also lead to lower cooling power of the battery.

When attempting to evaluate the possible impact that the improved battery usage may bring to prolonging battery life, there are at least a few indicative factors to consider. According to [11], the effective Ah-throughput, Ah_{eff} , proportional to battery life, may be estimated as follows

$$Ah_{eff} = \sum w_E n_E Ah_E \quad (8.1)$$

where the index E denotes the event at which an Ah-throughput, Ah_E , is drawn. The factors w_E and n_E correspond to the severity of the event and the number of such events, respectively. This simple estimation may suggest that a 10.9 % average reduction in Ah-throughput would also increase the effective battery life by ~ 12.2 %. This is under the assumption that w_E and n_E are constant. However, with lowered RMS currents w_E would be lowered as well, suggesting further improvements of battery life.

According to [17], the charge rate of the battery can strongly influence its lifetime. As an example, the cycle life was increased by 100 % by reducing the charging rate from 3.75 C-rate to 2 C-rate, where C-rate corresponds to the current normalized with battery capacity. In this example it would be equivalent to fully charging the battery in 16 and 30 minutes respectively. This suggests that it may perhaps be more important to consider how quickly the battery is recharged between trips before analyzing the usage during actual driving. The observed improvement in battery operation during driving is likely to have a significant positive impact if the battery is also recharged slowly between each trip, whereas fast recharge induces more stress to the battery which may seriously limit the relative impact of this improvement.

8.3 Modeling errors

The quite coarse modeling of the ICE startup sequence has been identified as one issue that may induce errors. A modeling problem when the engine is started can be seen, for example in Figure 6.6 where the torque of the ICE is negative during startup. This could perhaps be due to incorrect modeling of the transmission control. Given that the ECMS solution turns the ICE on and off many times over a drive cycle, the loss will grow with the number of engine starts and become quite significant. The number of ICE startups aside, both discharge strategy implementations are using the vehicle model in similar ways, suggesting that modeling errors would have equivalent impact on both solutions and thereby cancel each other.

Another issue related to modeling may be the feedback gain of the simulated driver, which is modeled by a PID-controller. A potential problem may be that high power demands may trigger unnecessarily high and short peaks of battery power costs, causing the power split to shift to ICE propulsion more frequently. This problem may be solved by applying a time dependent ICE startup cost that decreases after some time once an engine start has been requested, or by decreasing the feedback gains in the driver model.

In the model used for the ECMS algorithm some power losses was neglected, such as the power losses in the transmission and the ISG inverter losses. If the

neglected power losses had been taken into account, the ECMS performance could perhaps have been improved.

8.4 Estimation of equivalence factor

As shown in Table 6.2, the equivalence factor is not very sensitive to the speed properties of the drive cycle but varies more depending on the trip length. Initial and final SoC levels affect the equivalence factor in the same way. By sweeping a larger set of drive cycles with ranging trip lengths and SoC limits, these parameters can present a clearer relation and help finding a function for a suitable s_0 to be determined. A better model for estimating s_0 may also reduce the fuel consumption further, due to less SoC feedback activity in $s(t)$. This is because SoC feedback can shade the normal cost calculation and thereby dismiss an otherwise good operating point for a less efficient one, simply due to temporary SoC deviation. It seems that the schedule used for selecting different ICE startup penalty costs is an effective complement to the equivalence factor in avoiding this problem.

8.5 Estimation errors

If the estimated value on the trip length D_{tot} is changed slightly, the result of the ECMS is also changed. This result was also proven in [3]. This means that if the exact trip length would have been used the fuel consumption could possibly have been reduced further. The distance was underestimated because it is not satisfying to end the trip with unconsumed battery energy that should have been used for propulsion.

9 Future work

Concepts and ideas that were either beyond time constraints to investigate or out of scope for the thesis but yet interesting for future developments of the solution are presented below.

9.1 Better engine start cost

One factor that showed to be of high importance for fuel consumption is the set of values used for the engine start penalty, P_{start} . When simulations were made to determine these values it was noticed that even small changes had a significant impact on the fuel consumption. There is still a large uncertainty in how close to optimal this variable startup cost is. This is mainly because it has been designed based on only two drive cycles in order to provide for validation and avoid “cycle beating” (specific drive cycle tuning). With a more sophisticated function for this penalty, preferably with inputs such as current SoC, speed and requested torque, a penalty more close to optimal could be estimated. It would be beneficial to couple this cost to the existing hardware (EM and ICE) and allow for easy modification with new system parameters when being applied into a different vehicle. This is because extensive tuning for every change of system is to be avoided.

9.2 Mechanical energy reference

Using distance to form the desired SoC discharge trajectory is not likely the best reference. As a part of future developments of the ECMS solution, the amount of information known a priori could perhaps be extended further. Information about the topography, expected speed limits and traffic situation for a specified trip between points A and B could be used to estimate the total mechanical energy required by the vehicle during the trip. By using the mechanical energy needed for propulsion as a basis for the SoC reference instead of the distance, it may be possible to achieve an even more efficient discharge path.

9.3 Route recognition

In order to aid the estimation of the mechanical energy reference mentioned before, some sort of route recognition method could be employed [3], unless the driver himself/herself feels like dialing the exact destination on the integrated GPS navigator. Based on logged data from earlier trips, some sort of route recognition algorithm can be used to find the most commonly occurring trips. Once a trip has been identified, information provided by services such as Google Maps® can be used to effectively estimate the trip length, time to travel and even the impact of traffic.

9.4 ECMS model update

An update of the ECMS model with the previously neglected losses from components such as ISG inverter, transmission efficiency, idle losses of the ICE as well as varying auxiliary power, could be done for a better evaluation of the ECMS control strategy.

The ISG should also be included in the ECMS algorithm so that an additional degree of freedom can be utilized, allowing further improvements in ICE operating point selection. This could bring benefits to battery operation by providing “cheap” recharge opportunities.

The ECMS algorithm uses *for*-loops and to be able to decrease the computational power, the loops can be exchanged to matrix operations. Some of the calculations in the algorithm can also be optimized for faster computations by using more efficient algorithms. Another impact of the computational power is how often the ECMS control should update the power split ratios. The updates are currently made every 10 ms. By lowering the update rate to e.g. 1 s, the result may provide faster computations. Further investigation of such a change should be made to see how it affects the accuracy of the model.

Another consideration that could be added to the ECMS algorithm is the various emissions; NO_x , CO_2 , CO , HC and particles. Also, for a more complete analysis of the impact of ECMS and blended mode discharge, the component wear, specifically in the ICE, should also be considered while formulating the cost function.

9.5 ECU implementation

The objective of real-time implementation for the ECU was not fulfilled. It would not be practical to transfer the current ECMS algorithm due to the long computational times required, but some investigation has been made of how such an implementation could be done. By using surface fitting algorithms, the ECMS optimization could be included in an ECU as lookup tables. There are toolboxes for surface fitting in MATLAB® for example the toolbox ARESLab [18], which can be used for generation of such surfaces.

10 Conclusions

Upon finishing the investigations of alternative strategies for control and discharge of electric energy in a hybrid powertrain, the following conclusions could be made.

- Fuel consumption was reduced by 4.2 % on average for all tested drive cycles with a blended discharge under ECMS control, compared to the rule-based CDCS discharge strategy, which is a satisfactory result. For the case of ECMS control with a CDCS discharge strategy, the fuel consumption was reduced by 1.0 % on average instead. Both figures reflect the corrected fuel consumption.
- An engine start penalty cost is important when it comes to reducing the number of engine starts and avoiding suboptimal operating points, which otherwise contributes to a higher fuel consumption. Consequently it is also important to consider the accuracy of the model during the engine start process.
- Battery power losses and Ah-throughput were reduced with the ECMS control strategy for both the CDCS and the blended discharge strategy. These are both beneficial for improving the battery life, especially if the recharge rate (current) from the grid is not too high.
- A less time consuming way of determining an equivalence factor was found, which is beneficial for large and complex simulation models.
- The speed segment layout of drive cycles had certain effects on the rule-based CDCS discharge strategy, where city driving first and highway afterwards (similar to NEDC) is significantly more beneficial than the other way around. With ECMS there is more robustness to such arrangements in the speed segment layout.

References

- [1] Vägverket, “Hållbart resande,” 2006. http://publikationswebbutik.vv.se/upload/1543/88587_hallbart_resande_utg_2.pdf Retrieved 2012-04-12.
- [2] Swedish Institute for Transport and Communications Analysis, “Res 2005-2006 the national travel survey,” 2007.
- [3] V. Larsson, “On discharge strategies for plug-in hybrid electric vehicles,” licentiate thesis, Signal and System, Chalmers University of Technology, Göteborg, Sweden, 2012.
- [4] A. Sciarretta, M. Back, and L. Guzzella, “Optimal control of parallel hybrid electric vehicles,” *IEEE Transactions on Control Systems Technology*, vol. 12, pp. 352–363, May 2004.
- [5] C. Zhang and A. Vahidi, “Real-time optimal control of plug-in hybrid vehicles with trip preview,” in *American Control Conference*, pp. 6917–6922, 2004.
- [6] V. Freyermuth, E. Falles, and A. Rousseau, “Comparison of powertrain configuration for plug-in hevs from a fuel economy perspective,” *SAE International*, 2007.
- [7] L. Guzzella and A. Sciarretta, *Vehicle Propulsion Systems*. Berlin Heidelberg: Springer Verlag, 2nd ed., 2007.
- [8] Embedded Success dSPACE, “Targetlink ®.” <http://www.dspace.com/en/inc/home/products/sw/pcgs/targetli.cfm> Retrieved 2012-05-31.
- [9] B. He and M. Yang, “Optimization-based energy management of series hybrid vehicles considering transient behavior,” *Int. J. Alternative Propulsion*, vol. 1, no. 1, pp. 79–96, 2006.
- [10] T. van Keulen and et al., “Design, implementation, and experimental validation of optimal power split control for hybrid electric trucks,” *Control Engineering Practice*, vol. 20, pp. 547–558, 2012.
- [11] H. Wenzl and et al., “Life prediction of batteries for selecting the technically most suitable and cost effective battery,” *Journal of power sources*, vol. 144, pp. 378–384, 2005.
- [12] C. Musardo and G. Rizzoni, “A-ECMS: An adaptive algorithm for hybrid electric vehicle energy management,” in *44th IEEE Conference on Decision and Control*, vol. 11, pp. 1816–1823, Oct. 2005.
- [13] D. S. Naibu, *Optimal Control Systems*. CRC Press LLC, 1st ed., 2003.

- [14] S. Stockar, V. Marano, M. Canova, and G. Rizzoni, “Energy-optimal control of plug-in hybrid electric vehicles for real-world driving cycles,” *IEEE Transactions on vehicular Technology*, vol. 60, no. 7, pp. 2949–2962, 2011.
- [15] P. Tulpule, V. Marano, and G. Rizzoni., “Energy management for plug-in hybrid electric vehicles using equivalent consumption minimisation strategy,” *Int. J. Electric and Hybrid Vehicles*, vol. 2, no. 4, pp. 329–350, 2010.
- [16] L. Johannesson, S. Pettersson, and B. Egardt, “Predicted energy management of a 4QT series-parallel hybrid electric bus,” *Control Engineering Practice*, vol. 17, no. 12, pp. 1440–1453, 2009.
- [17] J. Groot, “State-of-health estimation of li-ion batteries: Cycle life test methods,” licentiate thesis, Energy and Environment, Chalmers University of Technology, Göteborg, Sweden, 2012.
- [18] G. Jekabsons, “ARESLab: Adaptive regression splines toolbox for matlab/octava,” 2011. <http://www.cs.rtu.lv/jekabsons/> Retrived 2012-04-24.

Appendices

A Drive cycles

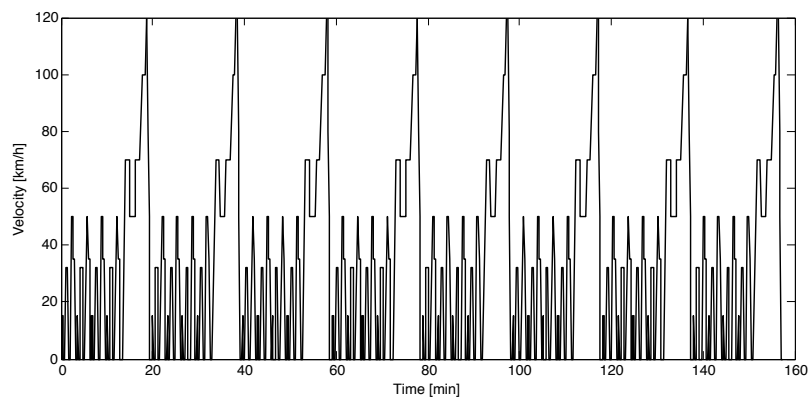


Figure A.1: Trip 1. New European Drive Cycle (NEDC), repeated 8 times, with predicted driving distance of 80 km.

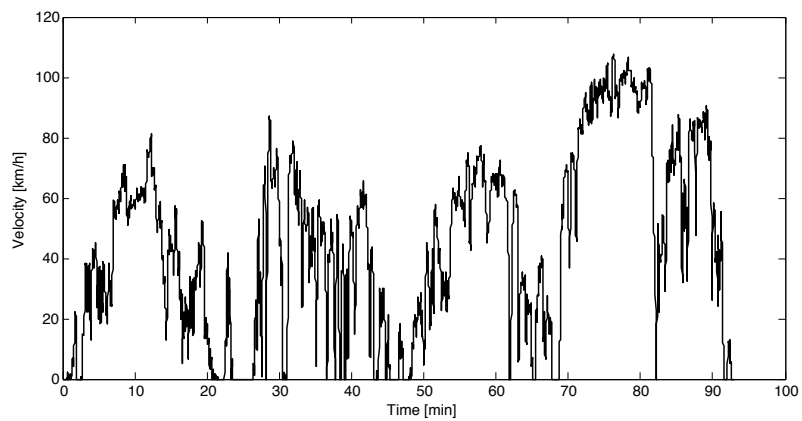


Figure A.2: Trip 2. Logged cycle with a predicted driving distance of 67 km.

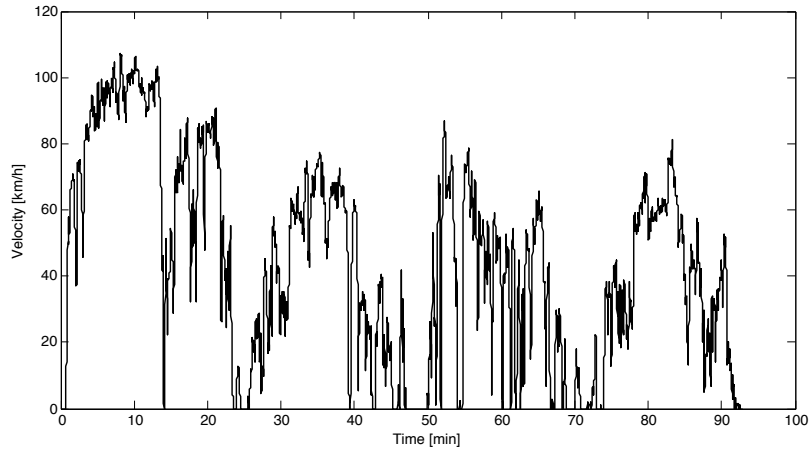


Figure A.3: Trip 3. Logged cycle with a predicted driving distance of 67 km. This drive cycle contains the same profile as Trip 2, but the high speed segment is placed to the beginning instead.

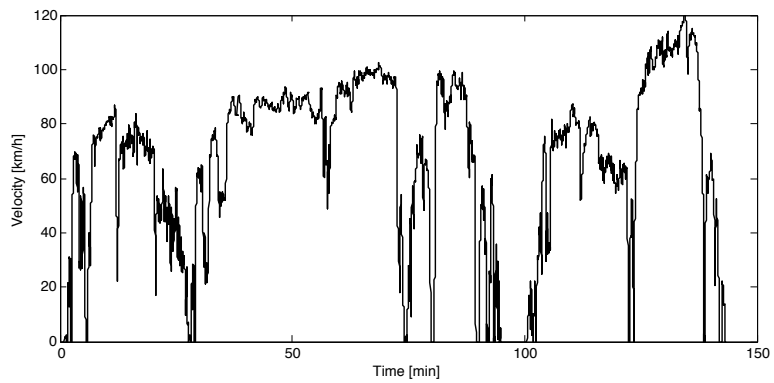


Figure A.4: Trip 4. A logged drive cycle with a predicted driving distance of 156 km.

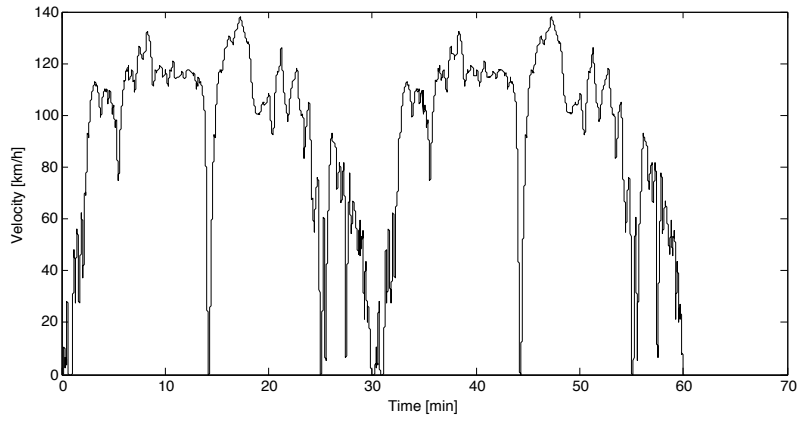


Figure A.5: Trip 5. Logged highway cycle with predicted driving distance ~ 92 km.

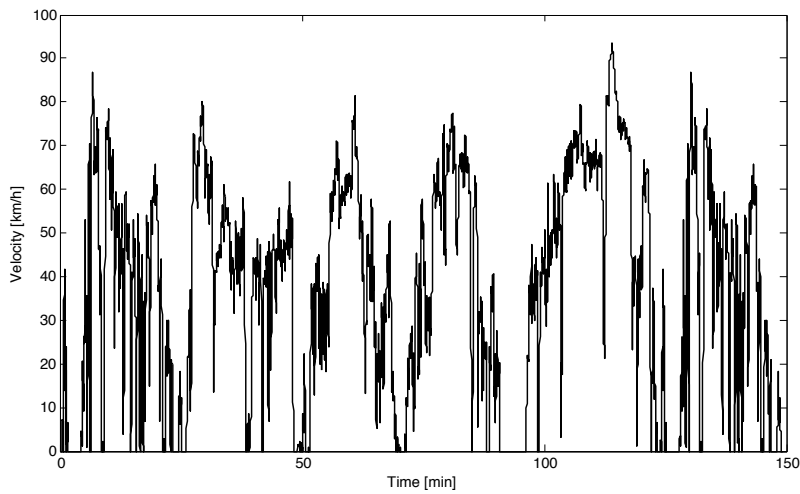


Figure A.6: Trip 6. Logged cycle with predicted driving distance 92 km.

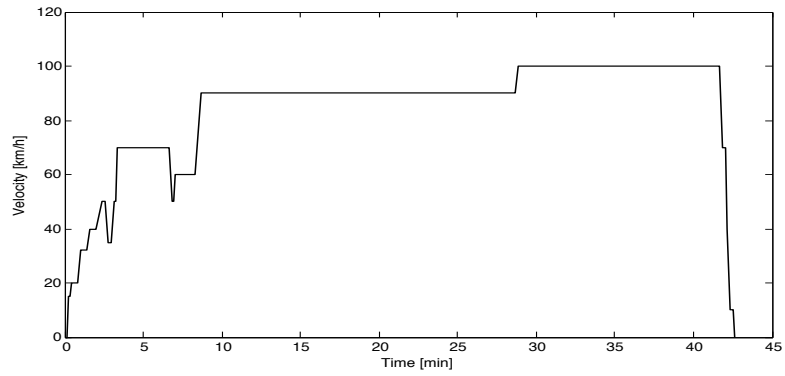


Figure A.7: Trip 7. Drive cycle used for evaluation with distance ~ 60 km.

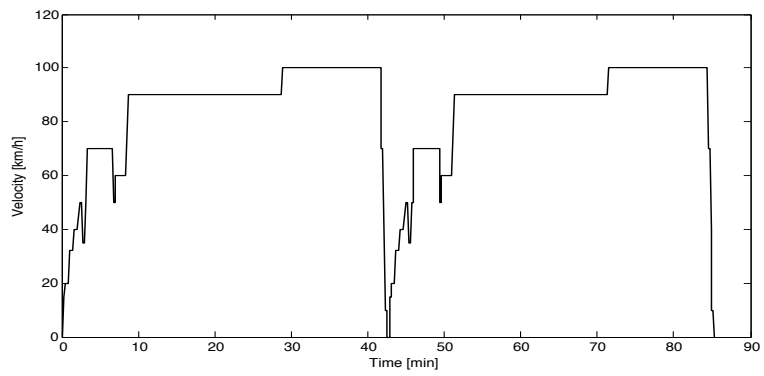


Figure A.8: Trip 8. Drive cycle used for evaluation with distance ~ 120 km.

B List of inputs and constants to the ECMS algorithm

| | |
|------------------|----------------|
| d | time dependent |
| D_{tot} | constant |
| SoC | time dependent |
| SoC_{final} | constant |
| SoC_{init} | constant |
| SoC_{ref} | time dependent |
| s_0 | constant |
| K | constant |
| T_{whl} | time dependent |
| ω_{whl} | time dependent |
| P_{aux} | constant |
| gr_{GB} | time dependent |
| gr_{EM} | constant |
| gr_{belt} | constant |
| $\eta_{gr,EM}$ | constant |
| $\eta_{gr,belt}$ | constant |
| \dot{m}_{fuel} | lookup table |
| $P_{batt,loss}$ | time dependent |
| $P_{fuel,start}$ | constant |
| $P_{EM,El}$ | time dependent |
| $P_{ISG,El}$ | time dependent |
| P_{aux} | constant |
| $P_{fuel,ICE}$ | time dependent |
| P_{fuel} | time dependent |
| P_{batt} | time dependent |
| Q_{lhv} | constant |
| V_{batt} | time dependent |
| u_1 | constant |
| u_2 | constant |

C The variation of $s(t)$

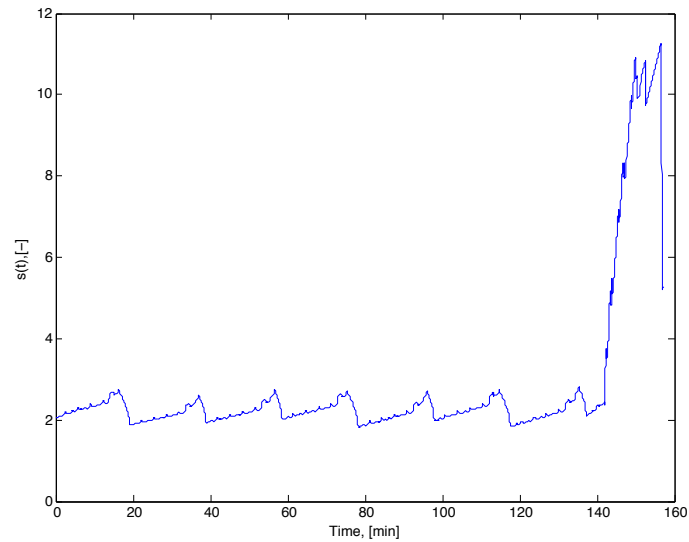


Figure C.1: $s(t)$ for Trip 1. The predicted trip length is shorter than the true one, therefore the large changes at the end of the trip.

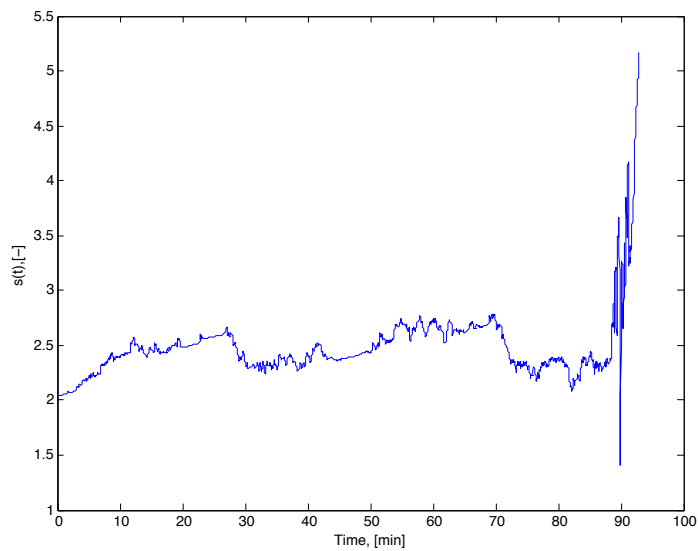


Figure C.2: $s(t)$ for Trip 2. The predicted trip length is shorter than the true one, therefore the large changes at the end of the trip.

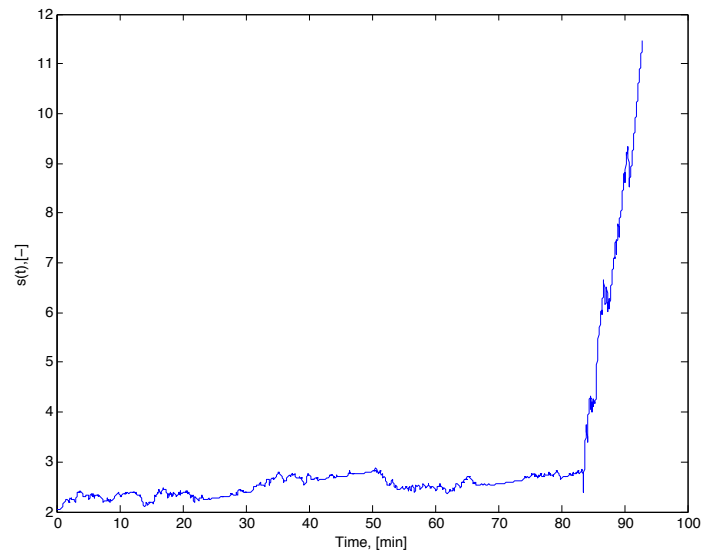


Figure C.3: $s(t)$ for Trip 3. The predicted trip length is shorter than the true one, therefore the large changes at the end of the trip.

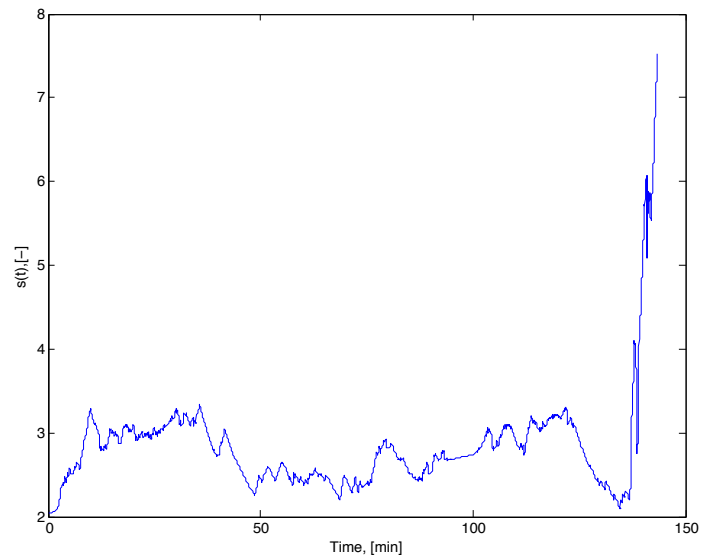


Figure C.4: $s(t)$ for Trip 4. The predicted trip length is shorter than the true one, therefore the large changes at the end of the trip.

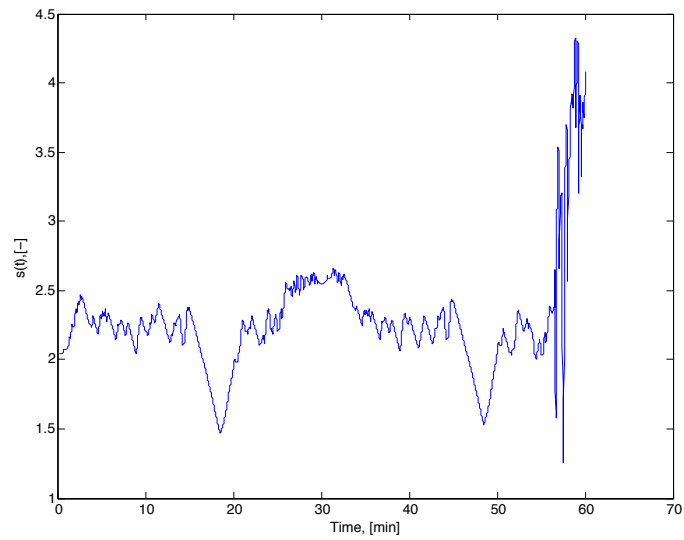


Figure C.5: $s(t)$ for Trip 5. The predicted trip length is shorter than the true one, therefore the large changes at the end of the trip.

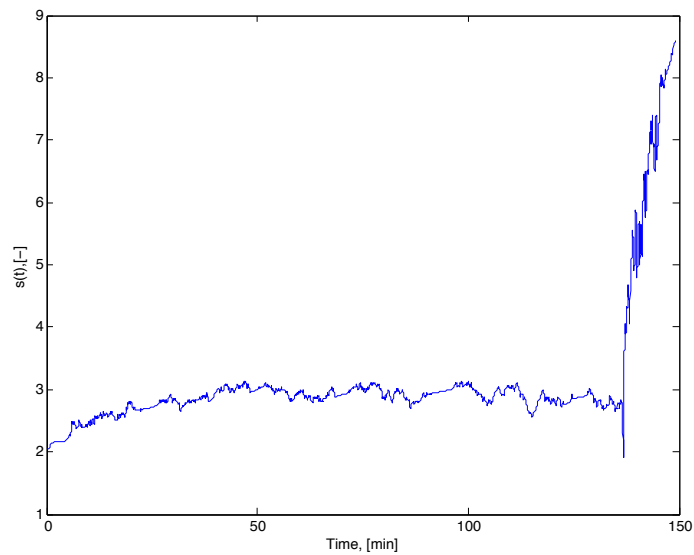


Figure C.6: $s(t)$ for Trip 6. The predicted trip length is shorter than the true one, therefore the large changes at the end of the trip.

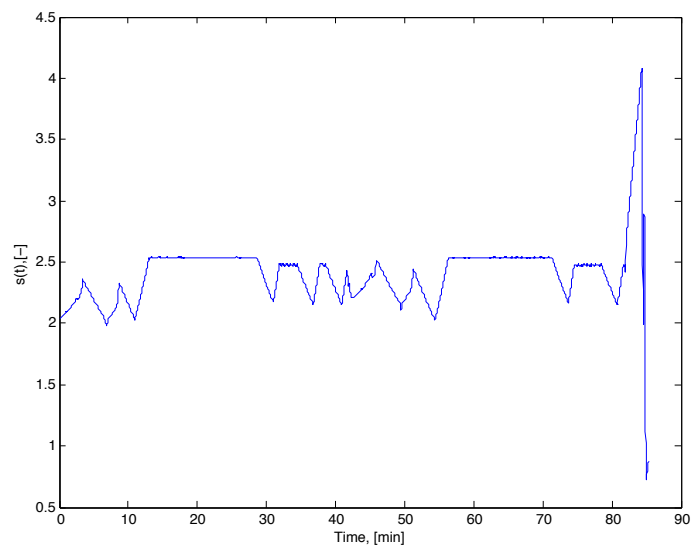


Figure C.7: $s(t)$ for Trip 7. The predicted trip length is shorter than the true one, therefore the large changes at the end of the trip.